DRD Line Item No. SE-7

DOE/JPL-954929-83/10

9950-876

INVESTIGATION OF ACCELERATED STRESS FACTORS AND FAILURE/DEGRADATION MECHANISMS IN TERRESTRIAL SOLAR CELLS

(NASA-CR-173757) INVESTIGATION OF ACCELERATED STRESS FACTORS AND FAILURE/DEGRADATION MECHANISMS IN TERRESTRIAL SOLAR CELLS Annual Report (Clemson Univ.) 121 p HC A06/MF A01 N84-28222

G3/44 Unclas 19840

FOURTH ANNUAL REPORT

OCTOBER 1983

J.W. Lathrop

Department of Electrical and Computer Engineering

Clemson University, Clemson, SC 29631

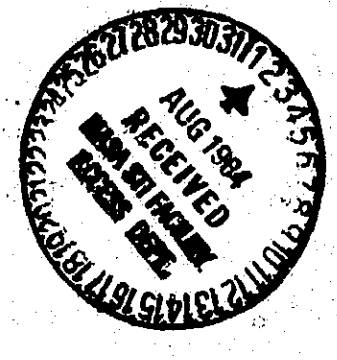

PREPARED FOR
JET PROPULSION LABORATORY

PREPARED BY
CLEMSON UNIVERSITY
CLEMSON, SOUTH CAROLINA 29631

DRD Line Item No. SE-7

DOE/JPL - 954929-83/10

ENGINEERING AREA

PHOTOVOLTAIC CELL RELIABILITY RESEARCH

INVESTIGATION OF ACCELERATED STRESS FACTORS AND FAILURE/DEGRADATION MECHANISMS IN TERRESTRIAL SOLAR CELLS

FOURTH ANNUAL REPORT

J.W. Lathrop

Department of Electrical and Computer Engineering
Clemson University, Clemson, SC 29631

October 1983

The JPL Flat-Plate Solar Array Project is sponsored by the U.S. Department of Energy and is part of the Photovoltaic Energy Systems Program to initiate a major effort toward the development of cost-competitive solar arrays. This work was performed for the Jet Propulsion Laboratory, California Institute of Technology by agreement between NASA and DOE.

CLEMSON PERSONNEL

Persons contributing to the work covered in this report include:

Dr. Jay W. Lathrop --	Principal Investigator
Mr. Dexter C. Hawkins --	Research Associate
Ms. Clara White Davis --	Graduate Student (Schottky barrier formation)
Mr. Konstantinos Misiakos --	Graduate Student (Schottky barrier formation)
Mr. Foster B. White --	Graduate Student (Sulfur dioxide tests) (Encapsulated cell testing)
Mr. H. Jarrett Cassell, Jr.--	Undergraduate Student
Mr. Thomas A. Bolin --	Undergraduate Student
Mr. Keith E. Summer --	Undergraduate Student
Mr. Paul Williamson --	Undergraduate Student
Mr. M. Lloyd Wright --	Undergraduate Student

ACKNOWLEDGEMENT

The Jet Propulsion Laboratory Technical Manager for this work was Mr. Edward L. Royal. His assistance in acquiring test samples and in supplying technical guidance to the program is gratefully acknowledged.

The assistance of Dr. R. G. Delumyea of the Clemson University Chemistry Department, who made many helpful suggestions concerning development of the sulfur dioxide test, is gratefully acknowledged.

ABSTRACT

This annual report presents results of an ongoing research program into the reliability of terrestrial solar cells. Laboratory accelerated testing procedures are used to identify failure/degradation modes which are then related to basic physical, chemical, and metallurgical phenomena. In the most recent tests, ten different types of production cells, both with and without encapsulation, from eight different manufacturers were subjected to a variety of accelerated tests. Results indicated the presence of a number of hitherto undetected failure mechanisms, including Schottky barrier formation at back contacts and loss of adhesion of grid metallization. The mechanism of Schottky barrier formation can be explained by hydrogen, formed by the dissociation of water molecules at the contact surface, diffusing to the metal semiconductor interface. This same mechanism can account for the surprising increase in sensitivity to accelerated stress conditions that was observed in some cells when encapsulated.

EXECUTIVE SUMMARY

This annual report is a summary of reliability research being conducted at Clemson University relating to failure/degradation mechanisms which can occur at the basic cell level. The research approach taken is to first detect the mechanical change and/or electrical degradation, which is charateristic of a particular cell construction, through the use of laboratory accelerated testing procedures, and then through detailed analysis to determine the basic physical, chemical, or metallurgical phenomena involved. In this report recent test results have been tabulated and the degradation mechanisms identified where possible for ten different unencapsulated state-of-the-art crystalline cell types from eight different manufacturers. Major program accomplishments are identified in this executive summary.

Schottky Barrier Contact Formation

Accelerated testing of unencapsulated cells uncovered a new degradation mechanism, not previously identified, affecting one type of cell construction. In this case degradation was accompanied by the formation of a distinctly non-linearity IV characteristic, primarily after exposure to bias-temperature testing, which greatly reduced the cell's maximum power output. It was concluded that a rectifying Schottky barrier had formed at the back contact. The particular cell construction where this was observed had a lightly doped substrate (no back surface field) and relied on a high concentration of surface states to give a low barrier height and consequent

ohmic contact. It is felt that atoms from the test environment, most likely hydrogen from dissociated water vapor, diffuse to the interface reducing the concentration of surface states. This increases the barrier height and results in a rectifying Schottky barrier. A series of additional controlled experiments to clearly define the role played by moisture in the Schottky barrier formation process is currently being planned.

Loss of Grid Adhesion

Another failure mode also detected from testing unencapsulated cells, which affected a different cell and whose cause is still under investigation, was the catastrophic loss of grid adhesion. Some loss of adhesion was noticed on other cell types, but not to this extent. The phenomenon affected all cells in a given lot and became so bad after a relatively short that a number of the tests had to be discontinued prior to their planned end point. Discussions with the manufacturer indicated the probable cause was contamination during processing and experiments are currently underway to determine if this is the case.

Enhanced Degradation of Encapsulated Cells

In addition to testing unencapsulated cells, nine of the cell types were tested as encapsulated single cell modules, which used different combinations of substrate, superstrate, and pottant materials. In all, seven different encapsulation configurations were involved. The encapsulated cells were subjected only to 85/85 and thermal cycle testing, however, because of a 100°C temperature limit on the organic pottant

materials used. A somewhat surprising result, which had been suspected as a result of earlier preliminary encapsulated cell testing, was confirmed by this present work -- encapsulated cells show appreciably greater degradation in many cases than unencapsulated cells. This is believed to be a result of the widely different penetration rates for water vapor molecules and their dissociation products, hydrogen and oxygen, in nonhermetic substrate materials. As a result, hydrogen and oxygen become trapped at the interface increasing the probability of one of these atomic species, most ikely hydrogen, diffusing to the silicon surface and changing the surface state density. As expected, however, encapsulation was found to offer protection against catastrophic mechanical type failures.

Little Protection Offered by Foil Substrates

Accelerated stress testing of encapsulated cells also showed that foil substrates behaved essentially the same as the non hermetic materials, i.e. they tended to increase cell degradation over what it was for unencapsulated cells. The phenomenon of trapping dissociation products at a metal - plastic boundary described above can also be used to explain this ineffectiveness of thin foil substrates. Hydrogen is able to diffuse through the foil whereas water vapor cannot. The only foil material tested was 1-mil aluminum and it is possible that other materials and thicknesses could provide better protection.

New Test and Analytical Facilities

An outdoor real time cell test facility is now in operation. Individual

cells, either encapsulated or unencapsulated, can be mounted on carriers, electrically measured under controlled conditions in the laboratory, and then attached to an outdoor inclined frame for long term environmental exposure. It is hoped that periodic remeasurement will detect degradation effects similar to those observed during accelerated testing and that correlation between the two mmethods can be established.

A new electron microscope analytical facility which will be devoted to semiconductor device reliability research is being constructed at Clemson. The facility will be an addition to Clemson's existing central electron microscope facility and will contain a high resolution (40 Å) scanning scope with x-ray wavelength dispersion and voltage contrast capability, and an Auger microprobe with scanning ion microprobe capability. The new instrumentation will be used to acquire quantitative information regarding cell degradation mechanisms. A workshop is planned for the spring of 1984 to acquaint the photovoltaic community with the topological and analytical capabilities of the facility.

TABLE OF CONTENTS

LIST OF FIGURES

LIST OF TABLES

1.0 INTRODUCTION

1.0 INTRODUCTION

This is the Fourth Annual Report on the Investigation of Accelerated Stress Factors and Failure/Degradation Mechanisms in Terrestrial Solar Cells, a photovoltaic cell reliability research program which has been conducted by Clemson University for the Flat-Plate Solar Array (FSA) Project of the Jet Propulsion Laboratories. The objective of the research is the determination of fundamental physical, chemical, and metallurgical phenomena which cause solar cells to degrade with time. The approach followed was to design laboratory test procedures which would accelerate anticipated field failure modes, and then to subject quantities of different types of commercially available cells to them. Testing was performed on both encapsulated and unencapsulated cells. The electrical and physical results of this testing could then be analyzed in an effort to identify the basic phenomena underlying the degradation. Corrective action would then be possible during manufacture to avoid the observed problem. The program was initiated in December of 1977 and earlier reports (1,2,3,4) have discussed many of the experimental and analytical methods employed, the data collected on several types of cells, and a number of preliminary conclusions. It is the purpose of this report to present the results obtained on the most recent group of cells which have undergone testing, to describe new degradation mechanisms and phenomena which were found, and to discuss new analytical methods currently under development.

As a result of their inherent simplicity, coupled with the lack of constraining specifications, solar cells are very reliable structures.

Verification of this degree of reliability is exceedingly difficult, however. Obviously accelerated testing is required which will result in measurable degradation in a reasonably short time, i.e. acceleration factors of 100 or more are required. Furthermore, as one moves progressively further away from the basic unencapsulated cell towards the finished photovoltaic array it becomes more difficult to increase the applied accelerating stresses without introducing extraneous failure modes and invalidating the test procedures. Section 3.0 of this report covers the first meaningful and systematic attempt to achieve accelerated degradation in encapsulated cells.

As verified by results obtained on the most recent group of cells, unencapsulated cell testing remains the most effective technique for producing significant degradation in sensitive cell types within a short time. Although absolute acceleration factors have not been determined, results are significant in their ability to differentiate between cell types. Although different failure/degradation modes were observed, many of the basic mechanisms behind these modes remain a mystery. On one particular cell construction, however, it was possible to interpret the observed maximum power degradation as being consistant with Schottky barrier formation at the back contact, as described in Section 4.2.

A first step towards establishing a relationship between accelerated test results and effects which occur in real time was begun during this reporting period. To accomplish this both encapsulated and unencapsulated single cells were mounted in outside racks and loaded at approximately the maximum power point. The individual cells were mounted in such a way that they could be removed for accurate measurement in the laboratory. It is

hoped that data accumulated in this way can be used to determine actual acceleration factors and to gain assurance that the same failure modes are being observed in the laboratory as in the field (Schottky barrier formation, for example).

During this round of testing many of the cell types in the test program were donated by manufacturers. In order to encourage this type of activity, Clemson acquainted each manufacturer, who contributed cells, with the accelerated test results of those cells as they occurred. Computer printouts of the electrical measurement data on appropriate cell types were mailed directly to the manufacturer, with as many as eight mailings being made to some manufacturers during the test period. Although some difficulty was encountered in establishing a routine for accomplishing this, it is felt the procedure was a success and should be continued.

2.0 ACCELERATED TESTING OF UNENCAPSULATED CELLS

PRECEDING PAGE BLANK NOT FILMED

2.0 ACCELERATED STRESS TESTING OF UNENCAPSULATED CELLS

2.1 Description of Cells

Since the program was initiated, 23 unencapsulated cell types from 12 different manufacturers have undergone some degree of stress testing. Table 1 summarizes, according to their primary metallizations, the 10 different unencapsulated types of cells from 8 different manufacturers that were in the latest group. Although the primary conductive metallization layer is the same for many of the cells, the barrier/strike layers which seperate it from the silicon may be quite different, both in composition and thickness. There are essentially four different layered conductor systems in use today -- copper plate, nickel plate, silver frit, and evaporated silver. The latter system is considered too expensive for present day terrestrial use and was not included in the present test group, although Ti-Pd-Ag cells have been tested in the past and found to be very reliable. The remaining three metallization categories may include a solder coating to help provide the necessary conductivity. The thick conductive layers could be easily identified, but more often than not the thin barrier/strike layers were unknown. Furthermore, the composition of and deposition methods for these layers vary from one manufacturer to another making it difficult to interpret the test results obtained on specific cell types in terms of generalized metallization systems. Photographs of the ten different cell types tested are shown in Figure 1. It can be seen that a wide variety of cell constructions, including EFG and dendritic ribbon were involved. Because the grid configurations of cell types are so distinctive, making it

TABLE 1.

UNENCAPSULATED CELL TYPES
CLASSIFIED BY PRIMARY METALLIZATION

CELL TYPE	CONDUCTING LAYER	SOLDER
N	nickel plate	yes
O	nickel plate	yes
P	nickel plate	yes
Q	nickel plate	yes
R	copper plate	no
V	copper plate	yes
W	nickel plate	yes
X	nickel plate	yes
Y	silver paste	no
Z	silver paste	no

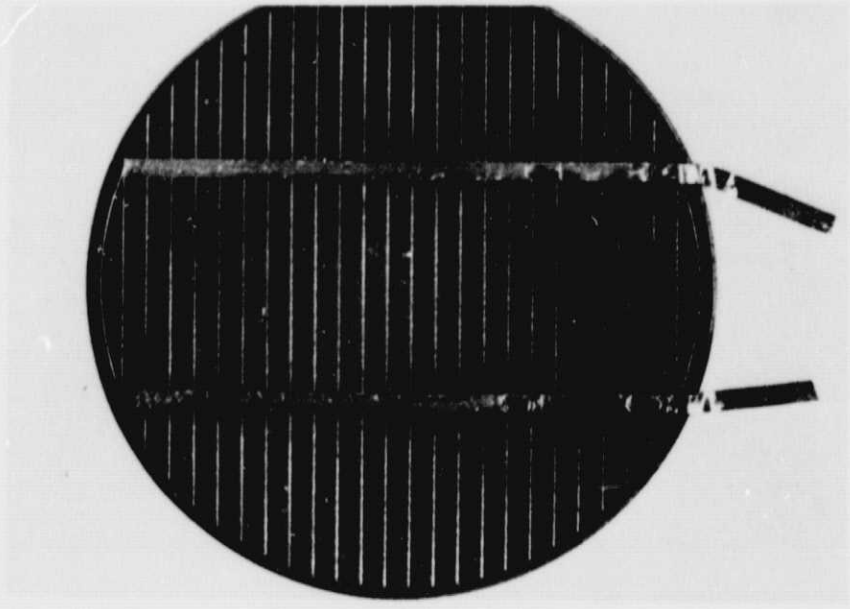

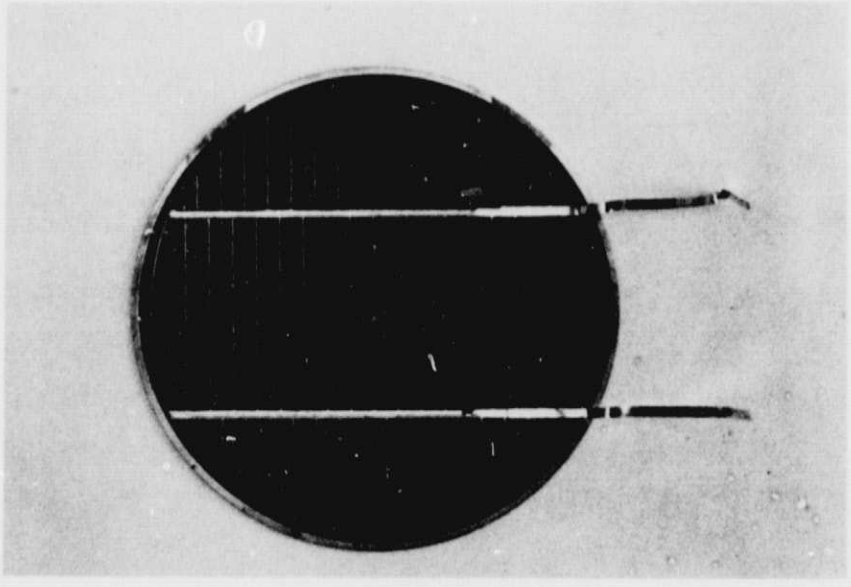

Figure 1. Cells in Unencapsulated Test Program

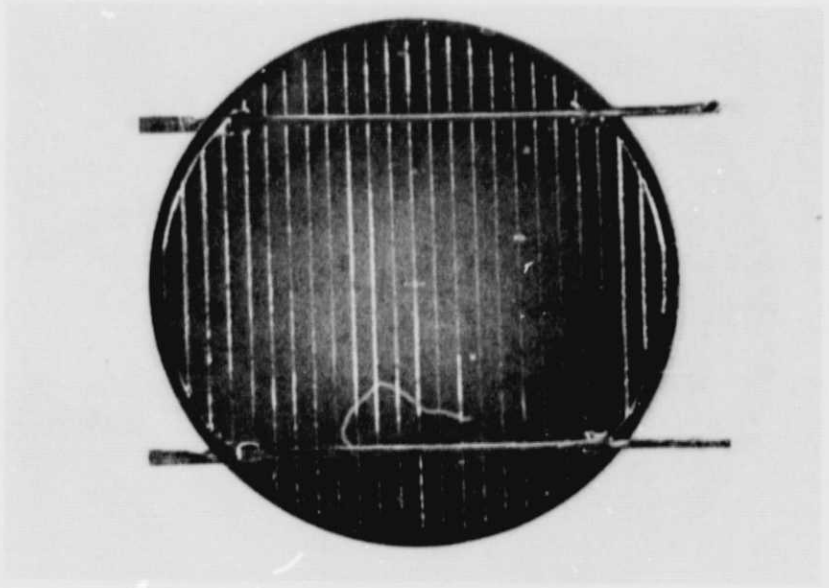

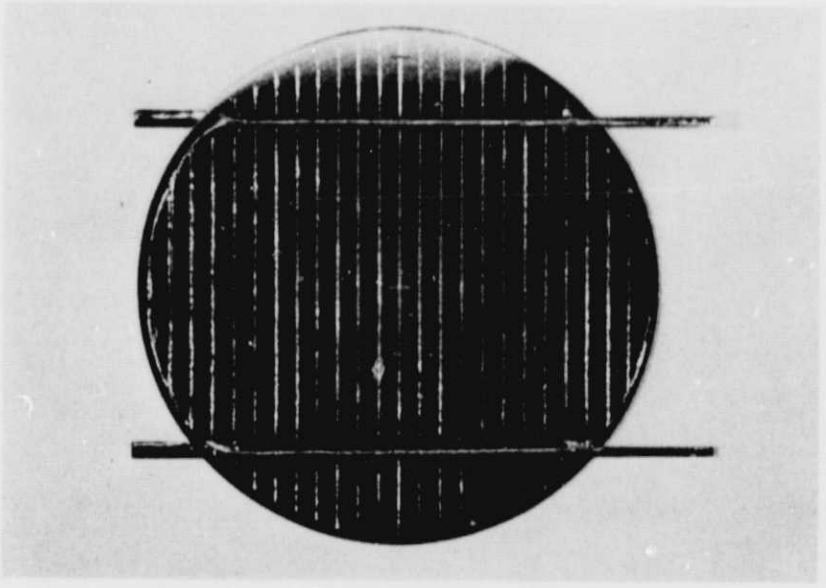

Figure 1 (continued). Cells in Unencapsulated Test Program
(Metallization difference only)

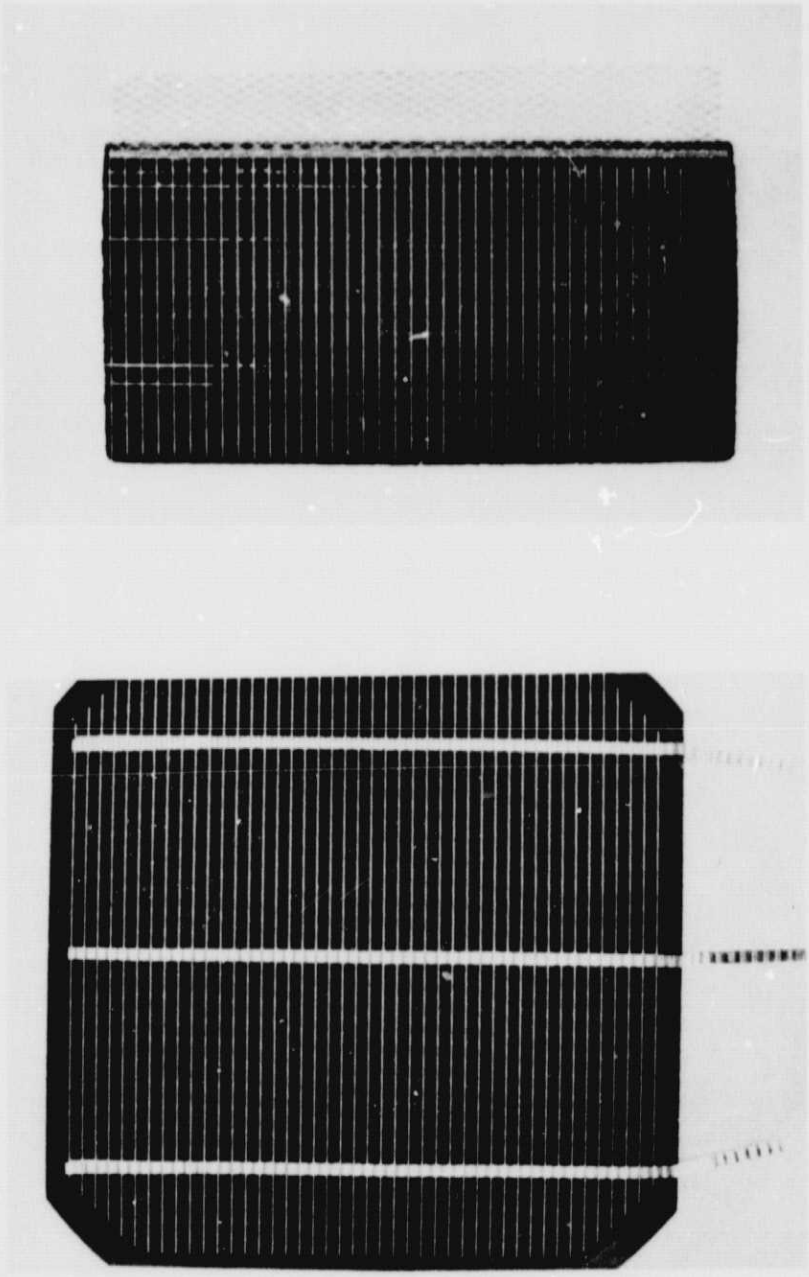

Figure 1 (continued). Cells in Unencapsulated Test Program

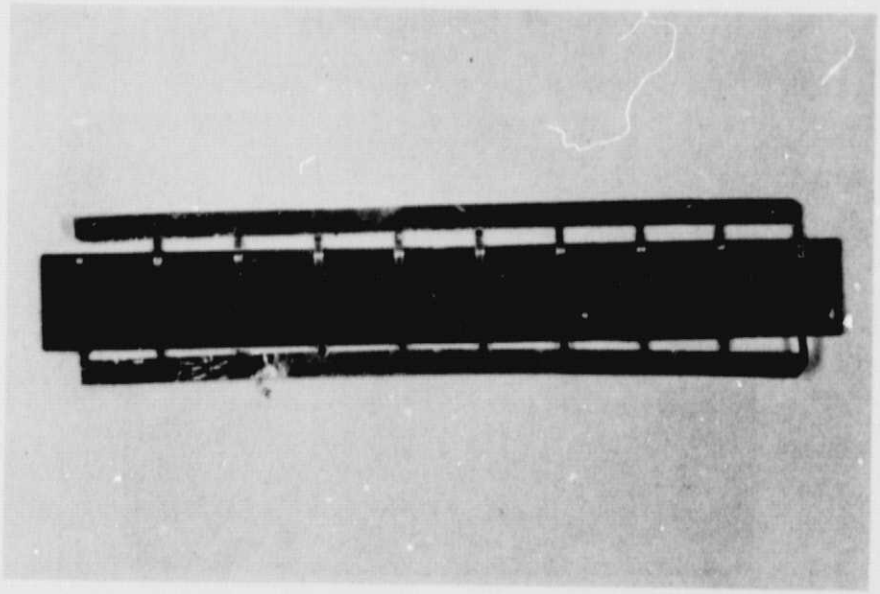

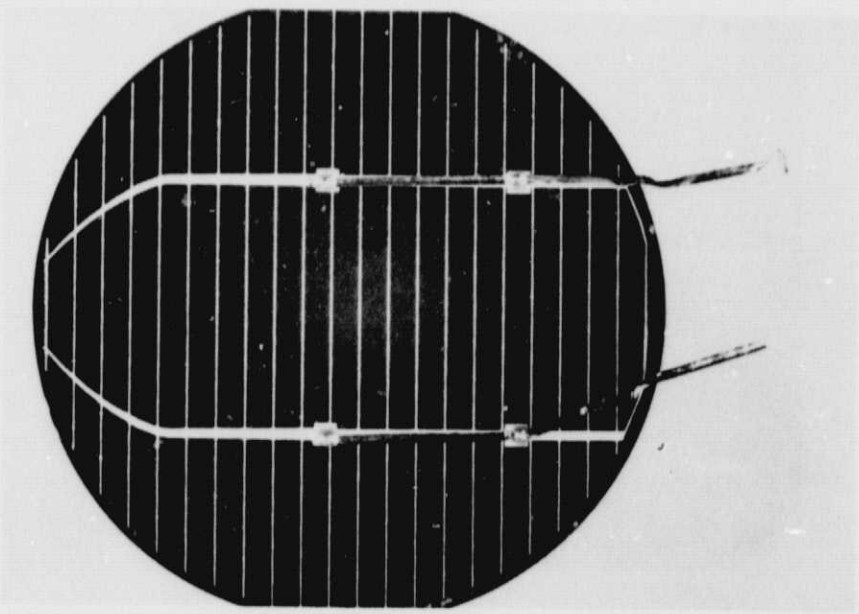

Figure 1 (continued). Cells in Unencapsulated Test Program

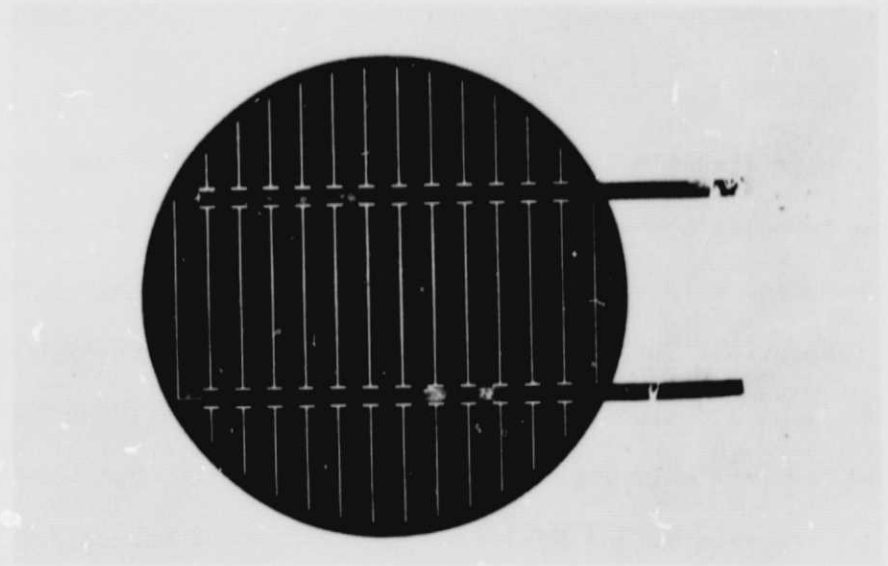

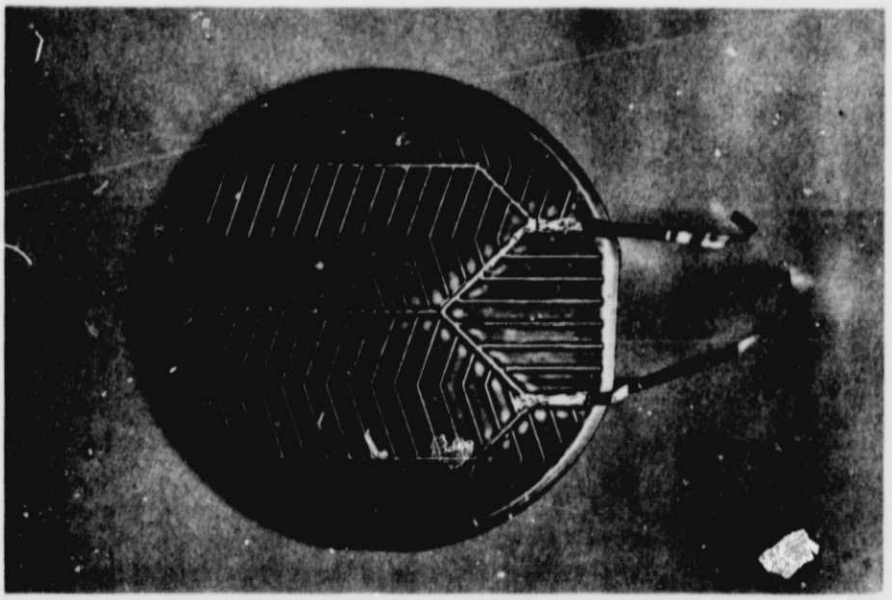

Figure 1 (continued). Cells in Unencapsulated Test Program

relatively easy to identify the manufacturer, these photographs have purposely not been correlated with the identifying letters used in the report.

Cells were visually inspected initially and at each downtime. Initial inspection revealed a continued improvement in quality over that for previous samples. Only one cell type showed any appreciable defects on incoming inspection. This cell, which was plated, apparently had masking which broke down and allowed spurious plating on the grid as shown in Figure 2. The nodules were only lightly attached to the cell, but were firmly attached to the grid lines. No uusual effects were observed during unencapsulated testing, but one cell with this defect showed increased degradation during testing when encapsulated.

2.2 Description of Tests

The cells were subjected to the standard Clemson accelerated test schedule for unencapsulated cells shown in Figure 3 (*). As indicated, there are 7 different tests, each having 4 down times. At the time of writing this report all cell types have not necessarily completed all down times, but tests are sufficiently far along that conclusions can be drawn with

---

* NOTE: The 75 C oven containing the N-, O-, P-, Q-, R-, and V-cells was allowed to overheat when first turned on because the student in charge of the test forgot to take into account heating due to biasing. Consequently the oven reached 150 C and remained there for approximately 24 hours. It is felt that this unfortunate occurrence accounts for the peculiar results seen in many of the cells where degradation was greater at 75 C than at higher temperatures. It is interesting that the reaction to this high temperature excursion, however, did not show up until a thousand hours later. When comparing cell types bear in mind that the X-, Y-, and Z-cells did not experience this excursion.

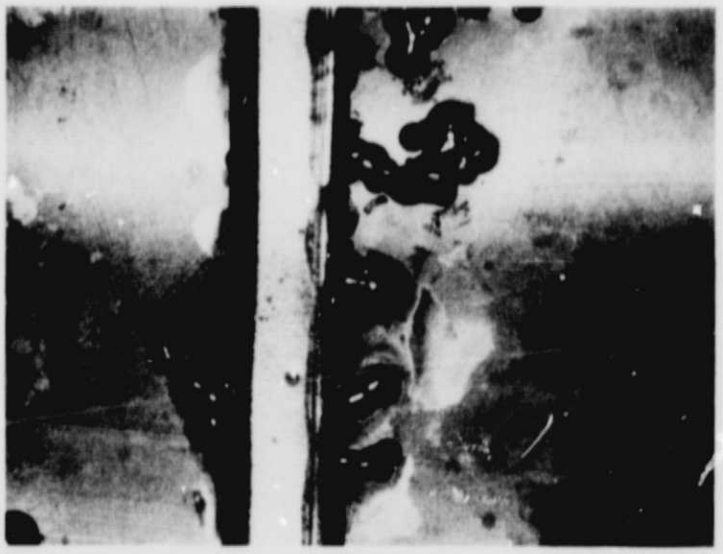

a) Light Field

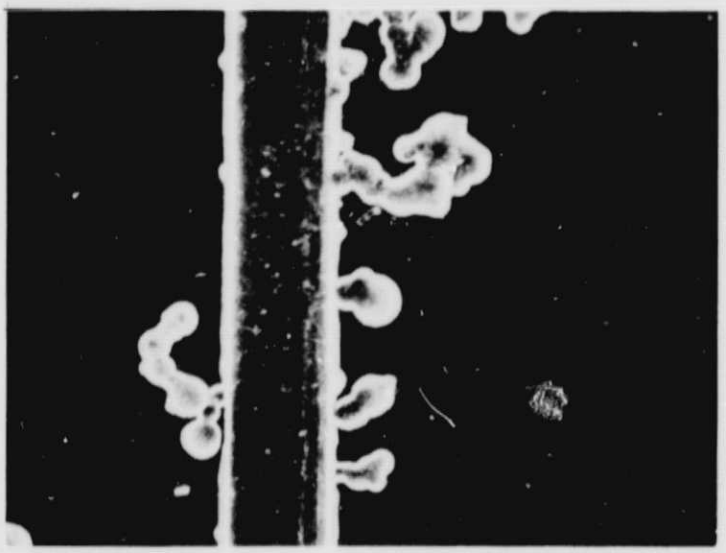

b) Dark Field

Figure 2. Photographs of Initial Plating Defects
(40 x)

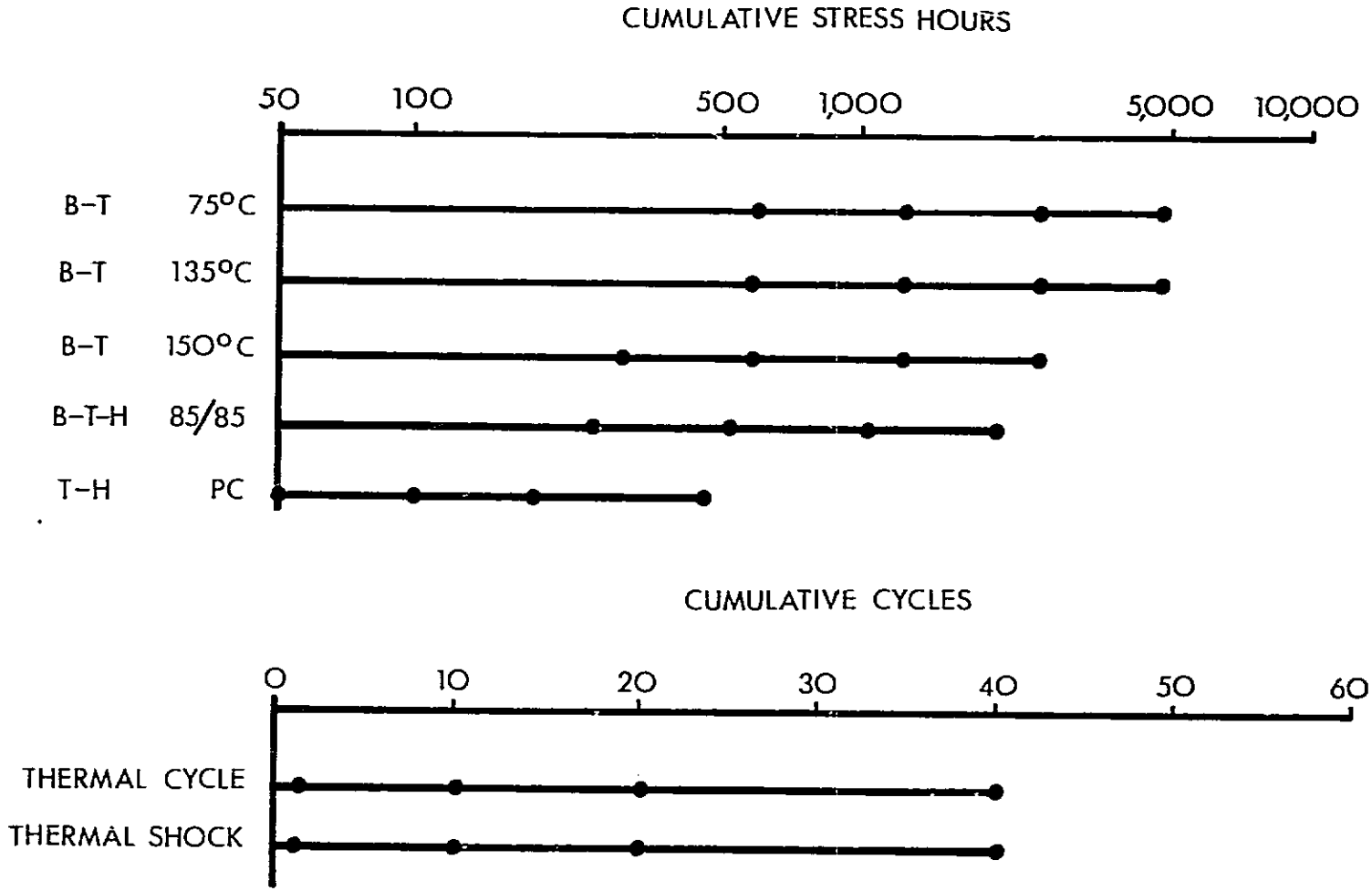

Figure 3. Clemson Accelerated Test Schedule for Unencapsulated Cells

confidence. Initially, and at each down time, the cells were electrically measured and visually inspected. Electrical measurement consisted of acquiring the IV characteristic curve and from it determining the parameters Pm, Isc, Vm, Im, and Voc. Although the series and shunt resistances were not specifically measured, the shape of the characteristic curves was qualitatively inspected for non-linearity. The IV characteristic taken at each measurement was saved in digital form for later retrieval if desired. The measurement system, which is capable of measuring parameters to 1% repeatability, is described in detail elsewhere (3,5). Of the electrical parameters, the maximum power output of the cell, Pm, is obviously the most useful in the measurement of degradation.

Visual defects which occurred as a consequence of testing, and which perhaps were exacerbated by handling, were detected by normal viewing procedures without the aid of magnification. The defects so detected were placed in one of the following four catagories:

leads

grid contact

back contact

cell fracture

Of these, the grid and back contact catagories are considered more serious from a practical standpoint that the other two, because leads and cell fractures are exacerbated by handling during testing and at the same time will be protected in the field by encapsulation to a greater extent. Defects relating to each of these areas were then characterized as:

0= no or very slight defect

1= moderate defect

2= severe defect (inoperative)

2.3 Test Results

2.3.1 General -- A number of things can happen to Pm, the maximum output power, when cells are subjected to accelerated testing. The following is a partial list:

1. Essentially no change

   Individual cells show only random changes of less than 3%

2. Uniform change

   All cells show about the same amount of degradation

3. Random change

   Some cells show large degradation while others in the same lot show slight or no change.

4. Progressive change

   Cells show increased degradation with increased test time.

5. Plateau effect

   Degradation levels out and does not decrease further with time.

6. Threshold effect

   No change to some point in time where a large change occurs.

From an analytical standpoint it would be desireable to have the test lots characterized as type-2. This would provide confidence that the

test was uncovering a single well defined failure mode. Unfortunately many test lots are type-3, making interpretation difficult. Often randomness (type-3), the plateau effect (type-5), and the threshold effect (type-6) can be explained by simultaneously observing catastrophic behavior, such as leads missing, fractures, loss of metal adherence, etc. When a lead comes off, for example, the output power will suddenly decrease, but will not change further with time, assuming that the remaining leads remain attached. Because the number of cells of any one type in each test was small (maximum of 25), such random behavior does not lend itself readily to quantitative data reduction methods, such as might yield a "one number" reliability figure of merit. In order to be able to interpret the data, failure modes caused by accelerated testing have been divided into two categories:

electrical degradation

catastrophic mechanical change

Electrical degradation is defined as a gradual and progressive change (usually a decrease) in Pm with no related visual effects (type-2 behavior). Examples of phenomenon which result in electrical degradation would be Schottky barrier formation at a contact and lifetime reduction through metal diffusion. Catastrophic mechanical change is defined as visually detectable change which would be expected to result in loss of power output, and which frequently can be characterized as "sudden". Examples would be loss of a lead, loss of grid adherence, and cell fracturing. Visual changes which were cosmetic, but which nevertheless might ulitmately lead to, or be related to, power loss were noted, but were not considered to be a primary part of the data analysis since the eventual results would show up as either Pm

degradation or as mechanical effects. Examples of cosmetic changes would be metal discoloration and solder bump formation.

In this report both accelerated test electrical measurement data and visual data are presented in a series of tables. Most cell types simultaneously exhibit both electrical degradation and mechanical changes. In an effort to seperate the two catagories, an effort has been made to remove the effect of mechanical change from the degradation tables. This explains, for example, why the table describing the 150 °C B-T test, which nominally has 20 cells, may show a lesser total number of cells as the test progresses. For the most part only the data relating to cells which experienced catastrophic change was removed from the table summaries -- the cells themselves continued to undergo testing. An exception to the procedure of removing the data for mechanically damaged cells involved thermal cycle and thermal shock testing, which would be expected to introduce only catastrophic type changes because of the short test times involved. In these cases no attempt was made to remove data since only a single failure mode catagory was expected.

2.3.2 Bias-Temperature Testing -- The electrical degradation results of bias-temperature testing are given in Table 2. The reader is urged to examine this table closely and note the regular progression of degradation with time and temperature for most cells and to note also the differences which exist between cell types. One cell type, the Q-cell, showed severe electrical degradation which was interpreted as being due to Schottky barrier formation at the back contact. This is discussed in detail in Section 4.2. Catastrophic mechanical changes are shown in Table 3. Two cell types, the X- and Z-cells showed severe mechanical problems during B-T

TABLE 2A
UNENCAPSULATED CELL BIAS TEMPERATURE TEST RESULTS
MAXIMUM POWER OUTPUT N-, O-, AND P-CELLS

Cell	Temp C	Time (hr)	Total Cells	Range of Maximum Power Degradation					
				0-2%	3-9%	10-19%	20-29%	30-49%	50-100%
N	75	600	25	23	2				
		1200	25	3	8	4	10		
		2400	25	4	7	4	9	1	
		4800			test in progress				
N	135	600	20	19	1				
		1200	20	19	1				
		2400	19	14	5				
		4800			test in progress				
N	150	300	19	15	4				
		600	18	11	7				
		1200	15	5	8	2			
		2400	14	3	6	4	2		
O	75	600	25	19	6				
		1200	24		9	10	3	2	
		2400	24		9	10	2	3	
		4800			test in progress				
O	135	600	20		14	6			
		1200	20		9	10	1		
		2400	20		6	12	2		
		4800			test in progress				
O	150	300	20		14	6			
		600	20		9	11			
		1200	19		3	10	5	1	
		2400	17			1	1	12	3
P	75	600	25	17	8				
		1200	24	15	8	1			
		2400	24	19	5				
P	135	600	20	15	5				
		1200	20	18	2				
		2400	20	17	3				
P	150	300	20	20					
		600	20	20					
		1200	20		data erratic				
		2400	19	7	10	2			

TABLE 2B
UNENCAPSULATED CELL BIAS TEMPERATURE TEST RESULTS
MAXIMUM POWER OUTPUT Q-, R-, AND V-CELLS

Cell	Temp C	Time (hr)	Total Cells	Range of Maximum Power Degradation 0-2%	3-9%	10-19%	20-29%	30-49%	50-100%
Q	75	600	25	2	23				
		1200	25					2	23
		2400	24					2	22
		4800		test in progress					
Q	135	600	20		1	16	3		
		1200	20			12	7	1	
		2400	20				2		18
		4800	20	test in progress					
Q	150	300	20		2	12	6		
		600	20			5	10	4	1
		1200	20						20
		2400		test in progress					
R	75	600	20	13	7				
		1200	15	10	5				
		2400	10	5	5				
		4800		test in progress					
R	135	600	16	10	6				
		1200	16	11	5				
		2400	14	4	8	2			
		4800		test in porogress					
R	150		test not run because of lack of samples						
V	75	600	23	21	2				
		1200	15	3	11	1			
		2400	interpretation difficult because of mechanical defects						
		4800		test in progress					
V	135	600	17	17					
		1200	17	14	3				
		2400	15	9	6				
		4800		test in progress					
V	150	300	20	18	2				
		600	16	15	1				
		1200	14	7	7				
		2400	interpretation difficult because of mechanical defects						

TABLE 2C
UNENCAPSULATED CELL BIAS TEMPERATURE TEST RESULTS
MAXIMUM POWER OUTPUT W-, AND X-CELLS

Cell	Temp C	Time (hr)	Total Cells	Range of Maximum Power Degradation 0-2%	3-9%	10-19%	20-29%	30-49%	50-100%
W	75	600	25	24	1				
		1200	25	6	19				
		2400		test in progress					
		4800		test not yet started					
W	135	600	20	15	5				
		1200	20	17	3				
		2400		test in progress					
		4800		test not yet started					
W	150	300	20	17	3				
		600	20	17	3				
		1200	20	4	15	1			
		2400		test in progress					
X	75	600	25	25					
		1200	25	24	1				
		2400		test in progress					
		4800		test not yet started					
X	135	600		interpretation difficult because of mechanical defects					
		1200		interpretation difficult because of mechanical defects					
		2400		test in progress					
		4800		test not yet started					
X	150	300		interpretation difficult because of mechanical defects					
		600		interpretation difficult because of mechanical defects					
		1200		test discontinued because of mechanical defects					
		2400		test discontinued because of mechanical defects					

TABLE 2D
UNENCAPSULATED CELL BIAS TEMPERATURE TEST RESULTS
MAXIMUM POWER OUTPUT Y- AND Z-CELLS

Cell	Temp C	Time (hr)	Total Cells	Range of Maximum Power Degradation 0-2%	3-9%	10-19%	20-29%	30-49%	50-100%
Y	75	600	25	10*	15*				
		1200	25	12*	13*				
		2400			test in progress				
		4800			test not yet started				
Y	135	600	20		10*	9*	1*		
		1200	20		10*	9*	1*		
		2400			test in progress				
		4800			test not yet started				
Y	150	300	20	1*	9*	10*			
		600	20		9*	10*	1*		
		1200			test in progress				
		2400			test not yet started				
Z	75	600	19	8	11				
		1200	15	10	5				
		2400			test in process				
		4800			test not yet strated				
Z	135	600	16	16					
		1200	15	11	4				
		2400			test in process				
		4800			test not yet started				
Z	150	300			data unavailable				
		600	15	11	4				
		1200			test in process				
					test not yet started				

*NOTE: Y-cell Pm values represent increases rather than decreases!

TABLE 3
UNENCAPSULATED CELL BIAS TEMPERATURE TEST RESULTS
CATASTROPHIC MECHANICAL CHANGE

Cell	Temp	Total # in test	Defect Category -- M=moderate, S=severe							
			Leads		Fracture		Grid		Back	
			M	S	M	S	M	S	M	S
N	75	25	1				1			
N	135	19	2				1		4	
N	150	20		2			5		3	
O	75	25			1				1	
O	135	20			2				2	
O	150	20	9			2			4	
P	75	25	2		3	1	2			
P	135	20	3		2		1			
P	150	20	2		2	1				
Q	75	25	3	1	4	1				
Q	135	20	1		5				1	
Q	150	20	5		1					
R	75	25	16		11	2	7		22	
R	135	20	12	1	7	12	3	1	7	3
R	150		test not run because of lack of samples							
V	75	25			1	12	2			
V	135	20			3	5	1		1	
V	150	20			3	8	1		2	
W	75	25								
W	135	20				1	1			
W	150	20					2			
X	75	25					6		7	
X	135	20	1				20		20	
X	150	20	4	15			5	15		
Y	75	25	1					1		
Y	135	20	3							
Y	150	20	3		2					
Z	75	25			2	6				
Z	135	20	4			5				
Z	150	18	6		1	3				

testing. The X-cell rapidly lost grid metal adherence at 135 and 150 C, and the Z-cell fractured disasterously under normal handling. The term "severe", in regard to catastrophic mechanical change, has previously been defined to mean change which caused the cell to become inoperable, but an explanation is perhaps in order concerning the more nebulous term "moderate". Moderate change ranged from that which was easily discernable to anything less than inoperable. Consequently, it is possible for a cell to become quite damaged and still be termed moderate, as shown by the photographs of "moderate" defects illustrated in Figure 4.

Considering the data of Tables 2 and 3, a somewhat subjective ranking of the cells with regard to their sensitivity to B-T testing can be made. Above average sensitivity to the test implies a less reliable cell. Such a ranking is given below, together with an explanation for above average sensitivity.

CELL	RELATIVE SENSITIVTY TO B-T TESTS
N	-- behavior considered average
O	-- above average due to excess electrical degradation
P	-- well below average sensitivity
Q	-- well above average due to back contact Schottky barrier formation
R	-- above average due to cell fracture
V	-- behavior considered average
W	-- below average sensitivity
X	-- well above average due to loss of grid adherence
Y	-- above average due to excess electrical change with time even though change was to higher Pm.
Z	-- above average due to cell fracture

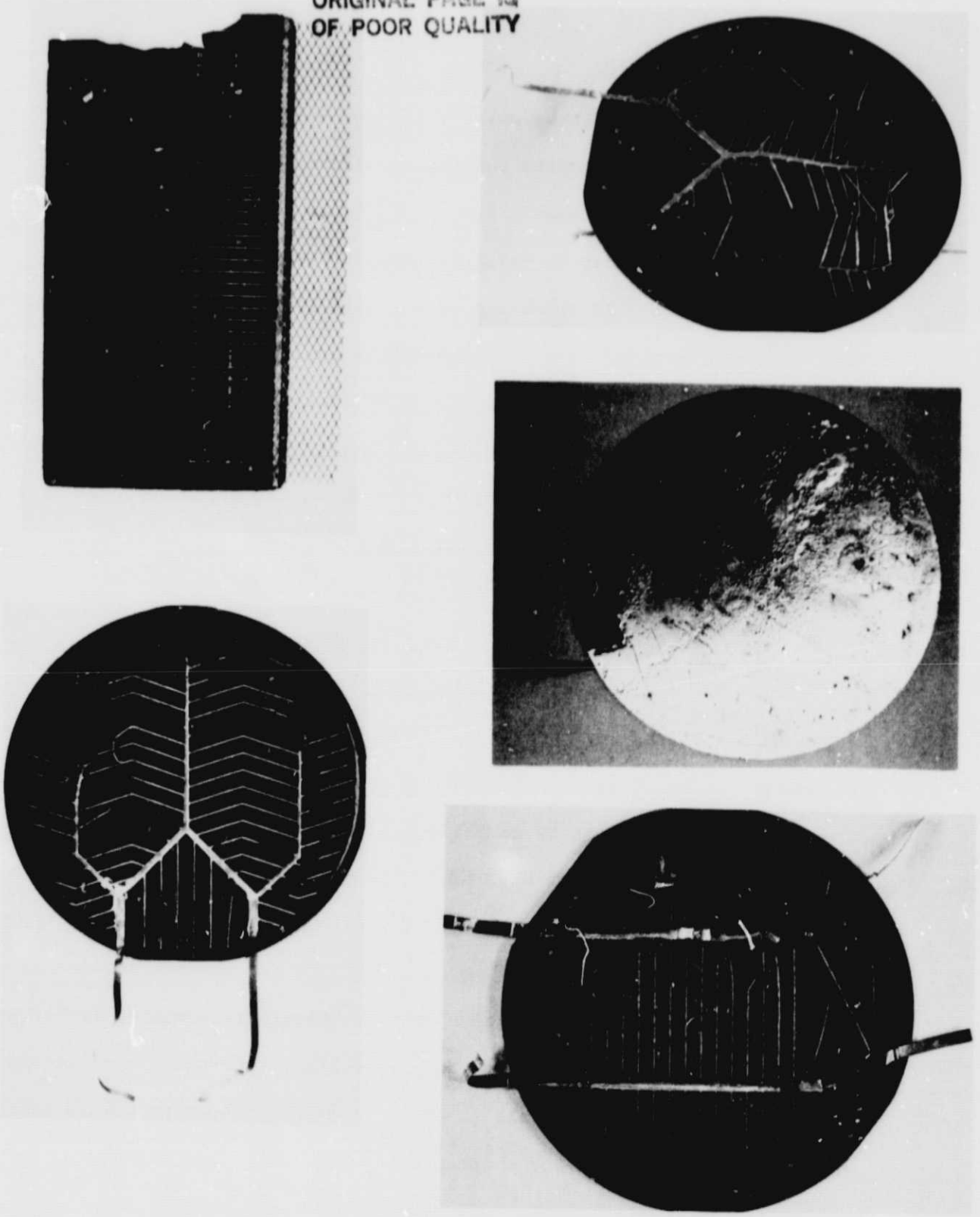

Figure 4. Examples of "Moderate" Mechanical Defects

2.3.3 Bias-Temperature-Humidity (85 C/85% RH) Testing -- Electrical degradation results for 85/85 testing are given in Table 4, and the catastrophic mechanical change results in Table 5. It is obvious that the 85/85 test in not nearly as severe a test as the B-T test. With the exception of the Q-cell the cells show little electrical degradation. This fact will be important to the discussion in Section 3 concerning the accelerated testing of encapsulated cells. Similarly, few mechanical effects were observed, but the X-cells which had severe grid adherence problems on B-T testing also had grid adherence problems in the 85/85 test. An overall ranking of cells in this test is not given because of the small changes that were observed.

2.3.4 Pressure Cooker (121 C/15 psig steam) Testing -- Electrical degradation results for pressure cooker testing are given in Table 6, and catastrophic change results in Table 7. It can be seen that the severity of the pressure cooker test is comparable to that of the B-T test. A regular progression of degradation with test time can be observed in a number of cases. The mechanical problems (loss of grid adhesion) associated with the X-cell were so severe that it was impossible to get any indication of non-mechanical related degradation. A particularly interesting effect was shown by the Y-cell which showed an astonishing improvement with testing. After 100 hours of testing all 10 of the Y-cells showed between 36 and 46% improvement in Pm, with the average being 42% ! An improvement had been observed during B-T testing, but not of this magnitude. No explanation is offered at the present time for the phenomenon, which had the effect of bringing cells having substandard performance more nearly in line with those

TABLE 4
UNENCAPSULATED CELL 85 C/85% RH TEST RESULTS
MAXIMUM POWER OUTPUT DEGRADATION

Cell	Time (hr)	Total Cells	Range of Maximum Power Degradation 0-2%	3-9%	10-19%	20-29%	30-49%	50-100%
N	250	11	4	7				
	500	11	3	7	1			
	1000	11	3	6	2			
	2000			test in progress				
O	250	14	14					
	500	14	11	3				
	1000	14	6	8				
	2000			test in progress				
P	250	13	11	2				
	500	12	6	5	1			
	1000	11	4	5	2			
	2000			test in progress				
Q	250	15	1	11	2			
	500	15		10	5			
	1000	14		2	12			
	2000			test in progress				
R			test not run because of lack of samples					
V	250	14	13	1				
	500	13	11	2				
	1000	12	11	1				
	2000			test in progress				
W	250	15	10	5				
	500	15	11	4				
	1000	15	1	14				
	2000			test in progress				
X	250	15	10	5				
	500	14	8	6				
	1000	13	11	2				
	2000	14	7	7				
Y			test not yet started					
Z			test not yet started					

TABLE 5
UNENCAPSULATED CELL 85 C/85% RH TEST RESULTS
CATASTROPHIC MECHANICAL CHANGE

Cell	Total # in test	Defect Category -- M=moderate, S=severe							
		Leads		Fracture		Grid		Back	
		M	S	M	S	M	S	M	S
N	15	3		1		2			
O	15								
P	15	3		3					
Q	15								
R		test not run because of lack of samples							
V	14							4	
W	15								
X	15	1				6			
Y	15	test in progress -- data not yet available							
Z		cells not tested							

TABLE 6
UNENCAPSULATED CELL PRESSURE COOKER TEST RESULTS
MAXIMUM POWER OUTPUT DEGRADATION

Cell	Time (hr)	Total Cells	Range of Maximum Power Degradation					
			0-2%	3-9%	10-19%	20-29%	30-49%	50-100%
N	50	8	6	2				
	100	6	4	2				
	200			test in progress				
	500			test not yet started				
O	50	10	4	3	3			
	100	10		5	4	1		
	200	10		5	1	3		1
	500			test in progress				
P	50	10			5	5		
	100	8			4	4		
	200			test in progress				
	500			test not yet started				
Q	50	10	3	6	1			
	100	10	1	6	3			
	200	10	1	3	3	1	1	1
	500			test in progress				
R			test not run because of lack of samples					
V	50	10	8	1	1			
	100	10	6	2	2			
	200			test in progress				
	500			test not yet started				
W	50	10	4	4	2			
	100	10	4	4	2			
	200			test in progress				
	500			test not yet started				

TABLE 6 (continued)
UNENCAPSULATED CELL PRESSURE COOKER TEST RESULTS
MAXIMUM POWER OUTPUT DEGRADATION

Cell	Time (hr)	Total Cells	Range of Maximum Power Degradation 0-2%	3-9%	10-19%	20-29%	30-49%	50-100%
X	50		interpretation difficult because of mechanical defects					
	100		interpretation difficult because of mechanical defects					
	200		interpretation difficult because ofmechanical defects					
	500		test terminated because of mechanical defects					
Y	50	10				2*	8*	
	100	10					10*	
	200	10				2*	8*	
	500		test in progress					
Z	50	8	8					
	100	8	8					
	200		test in progress					
	500		test not yet started					

*NOTE: Y-cell Pm values represent increases rather than decreases!

TABLE 7
UNENCAPSULATED CELL PRESSURE COOKER TEST RESULTS
CATASTROPHIC MECHANICAL CHANGE

Cell	Total # in test	Defect Category -- M=moderate, S=severe							
		Leads		Fracture		Grid		Back	
		M	S	M	S	M	S	M	S
N	10		1			2			
O	10			1					
P	10								
Q	10	1				2			
R		test not run because of lack of samples							
V	10			1					
W	10								
X	10	5	4			5	5		
Y	10	3							
Z	8								

of other cell types. The Y-cell metallization was printed silver and it is felt that some portion of the metallization fabrication cycle had not been properly optimized by the manufacturer as the effect is not generic to this type of construction. In keeping with standard reliability practice, however, any change -- even an improvement -- is viewed with suspicion, and consequently this cell was rated down because of this behavior.

A subjective ranking of cells regarding their sensitivity to pressure cooker testing results in:

CELL	RELATIVE SENSITIVTY TO PRESSURE COOKER TESTS
N	-- below average sensitivity
O	-- above average due to excess electrical degradation
P	-- above average due to excess electrical degradation
Q	-- above average due to excess electrical degradation
R	-- no tests planned due to lack of samples
V	-- average sensitivity
W	-- average sensitivity
X	-- well above average due to mechanical problems: loss of grid adherence and loss of leads
Y	-- well above average due to excess electrical change with time even though change was to higher Pm.
Z	-- below average sensitivity (preliminary)

2.3.5 Thermal Cycle (-65 C to + 150 C) Testing -- Electrical degradation results for thermal cycle testing are given in Table 8, and the catastrophic change results in Table 9. As was mentioned, the degradation results in this case include the effect of visual changes such as grid and lead loss. Thus from Table 8 it can be seen that the individual N-cells were either not affected by thermal cycling or they were drastically affected to the point where they lost 50% of their power output. From Table 9 it appears that the problem involved the loss of the back contact, presumably as a result of differential expansion coupled with weak adhesion. The Q-cells were plagued by the grid loss, as were the X-cells. This was a new failure

TABLE 8
UNENCAPSULATED CELL THERMAL CYCLE TEST RESULTS
MAXIMUM OUTPUT POWER DEGRADATION

Cell	Cycles #	Total Cells	Range of Maximum Power Degradation 0-2%	3-9%	10-19%	20-29%	30-49%	50-100%
N	1	10	9				1	
	10	10	8			1	1	
	20	10	6	1		1	2	
	40	10	5	1		1	2	1
O	1	10	10					
	10	10	3	7				
	20	10	1	5	4			
	40	10	1	1	6	2		
P	1	10	10					
	10	10	9	1				
	20	10	9	1				
	40	10	7	3				
Q	1	10	9	1				
	10	10	3	5		2		
	20	10		6	2		2	
	40	10			2	3	3	2
R	test not run because of lack of samples							
V	1	10	5	4	1			
	10	9	5	1	2	1		
	20	9	4	1	2	2		
	40	9	3	2	1	3		
W	1	10	5	5				
	10	10	1	7	1	1		
	20	10		3	5	1	1	
	40	10		1	5	3	1	
X	1	10	10					
	10	10	10					
	20	10	2	7	1			
	40	9				1	1	7
Y	1	10	10					
	10	10	8	1	1			
	20	10	6	1	2		1	
	40	10	2	4		1	1	2
Z	Test not run because of lack of samples							

TABLE 9
UNENCAPSULATED CELL THERMAL CYCLE TEST RESULTS
CATASTROPHIC MECHANICAL CHANGE

Cell	Total # in test	Defect Category -- M=moderate, S=severe							
		Leads		Fracture		Grid		Back	
		M	S	M	S	M	S	M	S
N	10							6	
O	10			7					
P	10	1		1		1		1	
Q	10	8		3		8		1	
R		test not run because of lack of samples							
V	10			3	1				
W	10			5					
X	10	2	1	1		10		7	
Y	10	7				2			
Z		test not run because of lack of samples							

mode for the Q-cells, but not for the X-cells. The V- and W-cells showed a more gradual and consistant degradation similar to that experienced in B-T testing. The only visible mechanical change was fracturing. The Y-cells showed considerable loss of power due primarily to lead loss. Soldering to silver screened metallization tends to be difficult and this type of failure mode has been observed before on other similar types of cells.

A subjective ranking of cells regarding their sensitivity to thermal cycle testing results in:

CELL	RELATIVE SENSITIVTY TO THERMAL CYCLE TESTS
N	-- above average due to loss of back contact
O	-- average sensitivity
P	-- below average sensitivity
Q	-- above average due to loss of grid adherence
R	-- no tests planned due to lack of samples
V	-- above average due to fracture
W	-- above average due to fracture
X	-- well above average due to loss of grid adherence
Y	-- above average due to lead loss
Z	-- test not yet started.

2.3.6 Thermal Shock (-65 C to 150 C) Testing -- Electrical degradation results for thermal shock testing are given in Table 10, and the catastrophic change results in Table 11. The electrical degradation results of Table 10 are almost an exact duplicate of those obtained during thermal cycling and reported in Table 8. This is not surprising as the two tests are similar in nature -- the difference being the rapidity with which the temperature is increased or decreased. It would be expected that thermal shock might cause more mechanical changes than thermal cycling since the rate of change of temperature is greater. From a comparison of Tables 9 and

TABLE 10

UNENCAPSULATED CELL THERMAL SHOCK TEST RESULTS
MAXIMUM OUTPUT POWER DEGRADATION

Cell	Cycles #	Total Cells	Range of Maximum Power Degradation 0-2%	3-9%	10-19%	20-29%	30-49%	50-100%
N	1	10	8	1	1			
	10	10	3	2	1	2	2	
	20	10	2	1		3	3	1
	40	9	1	1	1		3	3
O	1	10	6	4				
	10	10	2	5	3			
	20	10	2	5	3			
	40	10		3	5	1	1	
P	1	10	6	4				
	10	10	6	3			1	
	20	9	2	7				
	40	9	3	6				
Q	1	9	1	2	4	1	1	
	10		(data accidentally omitted)					
	20	9			2		3	4
	40	7			1	1		5
R			test not run because of lack of samples					
V	1	10	6	3	1			
	10	8	1	1	3	1	2	
	20	8		2		3	2	1
	40	5		1		2		2
W	1	10	1	7	2			
	10	10			4	5	1	
	20	10			2	4	3	1
	40	10				3	6	1
X	1	10	10					
	10	7					1	6
	20	6						6
	40		test discontinued					
Y	1	10	7	3				
	10	8	1	4	1		1	1
	20	7		3	2			2
	40	5		3	1	1		
Z			test not run because of lack of samples					

TABLE 11

UNENCAPSULATED CELL THERMAL SHOCK TEST RESULTS
CATASTROPHIC MECHANICAL CHANGE

Cell	Total # in test	Defect Category -- M=moderate, S=severe							
		Leads		Fracture		Grid		Back	
		M	S	M	S	M	S	M	S
N	10	2		2		1	1	3	
O	10			8				7	
P	10	1		4	1				
Q	10	6	2	8	1	6			
R		test not run because of lack of samples							
V	10			3	5			1	
W	10			10					
X	10		10	2			10	3	
Y	10	5	1		4				
Z		test not run because of lack of samples							

ll this appears to be the case.

All cell types fracture to some degree during thermal shock testing. The W-, Y-, and V-cells appear to be particularly susceptible. The X-cell has a severe problem with grid loss, a phenomenon that was also noticed in other tests (refer to Section 4.3). In addition, thermal shock resulted in severe lead loss for the X-cell. This particular cell had an extended lead contact, i.e. the lead made contact with the cell completely across the slice rather than only at one point near the edge. When lead loss occurred the silicon fractured under the metal lead so that it came loose with silicon still attached. An example of this type of failure is shown in Figure 5. The combination of these two failure modes was so severe that the test had to be discontinued after 20 cycles.

The W-cell showed very consistant and progressive electrical degradation. The routine inspections, while they showed some fracturing, did not seem to indicate any visual effect capable of producing such a consistant behavior and further study is warrented. The W-cell had also shown this same consistant and progressive behavior as a result of thermal cycle testing.

The liquid transfer thermal shock test is so drastic a test it is a wonder that all cells do not self destruct. One type, the P-cell was only relatively minimally affected by the test. Only one cell in the test lot showed appreciable degradation and it was due to a severe fracture. The P-cell also behaved the best during thermal cycle testing.

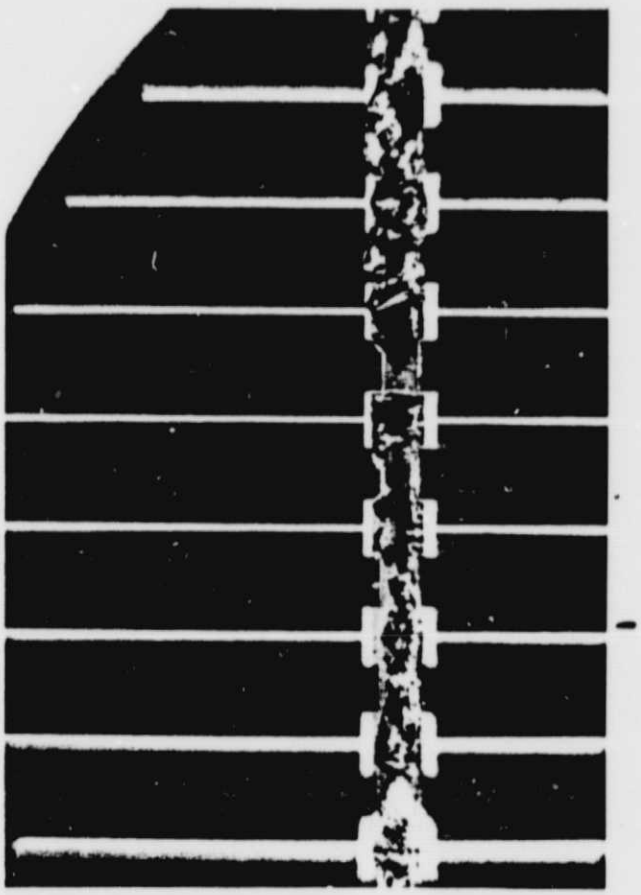

Figure 5. Photograph of Fracturing Under Lead as a Result of Thermal Shock Testing

A subjective ranking of cells regarding their sensitivity to thermal shock testing results in:

CELL	RELATIVE SENSITIVITY TO THERMAL CYCLE TESTS
N --	above average due to back contact problems
O --	average sensitivity
P --	well below average
Q --	obove average due to fracturing
R --	no tests planned due to lack of samples
V --	above average due to fracturing
W --	well above average due to electrical degradation
X --	well above average due to lead loss and grid failure
Y --	above average due to lead loss
Z --	no tests planned due to lack of samples

3.0 STRESS TESTING OF ENCAPSULATED CELLS

3.0 STRESS TESTING OF ENCAPSULATED CELLS

3.1 Introduction

As indicated in Section 2, accelerated stress testing of unencapsulated cells is able to delineate certain failure mechanisms which may affect cell life in field operation, such as Schottky barrier contact formation (non-linear IV characteristic) and loss of contact adherence. Cells in use, however, are not bare, but are encapsulated in modules and it is not evident what effect encapsulation will have on the failure modes observed during unencapsulated testing. Ideally it would be desireable to subject encapsulated cells to the same type of accelerated testing as unencapsulated cells. Previous work has shown, however, that because of the organic pottant materials involved, extraneous failure modes are introduced when temperatures higher than 100 C are used. The use of temperature as an effective acceleration factor is therefor severly limited once the cell has been encapsulated. However, it was felt that since encapsulation could be expected to primarily influence the rate of corrosion, either reducing it by limiting moisture penetration or increasing it by trapping moisture and chemical byproducts on the surface, that the 85/85 test would perhaps provide useful accelerated test information. Thermal cycling would be another potentially valuable accelerating test, provided the upper temperature did not exceed 100 C.

In order to see the effect of these two tests on cells which were encapsulated and to compare them with the unencapsulated test results,

Clemson contracted with Springborn Laboratories of Enfield, CT to fabricate a number of single cell modules, hereafter called coupons, using different cell types and different encapsulation configurations. The reader can gain an appreciation for the size and shape of the coupons by referring to Figure 10 which shows a number of different types assembled in an outdoor array. In addition to the Springborn samples, several manufacturers also supplied coupons of their cells. The result was the matrix of samples shown in Table 12. In this table each row refers to a different encapsulation configuration and each column to a different cell type and whether it was encapsulated by Springborn or by the cell manufacturer. Note that the manufacturer of the V-cell supplied coupons which included no substrate (G/EVA) and two different types of foil substrates (G/EVA/F1 and G/EVA/F2). (The designation F1 and F2 is only used to differentiate between these two types of coupons and does not imply that the F1 configuration is similar to those fabricated by Springborn Labs for the other cell types.) It can be seen that with the exception of the glass/silicone rubber/glass encapsulated Q-cells, which have yet to be started, all cells have completed the full 2000 hour test.

Testing of the encapsulated cells was more difficult and less "reliable" than testing unencapsulated cells for a number of reasons. For one thing, the coupons were physically bigger than the cells so that fewer were able to fit in a test chamber. Assembly of the coupons utilized non-standard, laboratory-like processes, involving components having widely differing thermal masses, with the result that curing cycles were not necessarily optimized. In fact the organic pottant material in several cells "ran" even though the stress temperature during test did not exceed

TABLE 12. Hours of 85/85 Testing Completed on Encapsulated Cell Coupons

	N	O	P	Q	Q	R	V	V	W	X	Y
COUPON	SPR	SPR	SPR	SPR	MFG	SPR	SPR	MFG	SPR	SPR	SPR
G/EVA	---	---	---	---	---	---	---	2000	---	---	---
G/EVA/T	2000	2000	2000	2000	---	---	2000	2000	---	2000	2000
G/EVA/F1	2000	---	2000	2000	---	2000	---	2000	2000	2000	2000
G/EVA/F2	---	---	---	---	---	---	---	2000	---	---	---
G/EVA/G	2000	---	2000	2000	---	---	---	---	---	2000	2000
G/EMA/T	2000	2000	2000	2000	---	---	2000	---	---	2000	2000
T/EVA/S	2000	2000	2000	2000	---	---	---	---	2000	---	2000
G/SR/G	---	---	---	---	TBS	---	---	---	---	---	---

--- = Tests not planned

SPR = Coupons fabricated by Springborn Laboratories

MFG = Coupons fabricated by cell manufacturers

TBS = To be started

G = glass, T = Tedlar, F = foil, S = steel, SR = Silicone Rubber

All tests are scheduled to end at 2000 hours

85 C. In this case pottant material dripped from the coupons leaving the cells directly exposed to the test ambient. These coupons were withdrawn from testing and samples sent to Springborn Laboratories where examination revealed incomplete curing of the polymer. Unfortunately there is no way to visually detect such improperly cured encapsulation prior to stress testing. It is therefore entirely possible that modules having similarly improperly cured encapsulation could be unknowingly deployed in the field unless adequate process controls are used. Loss of pottant does not automatically mean electrical degradation, however.

The expense of fabrication, coupled with limited test chamber size, restricted the number of coupons in a test to five or less. Hence it was difficult to obtain results which were statistically meaningful. Accurate electrical measurement was also more difficult than with unencapsulated cells. Temperature measurement and control was complicated and less accurate since the cell itself was inaccessible. Kelvin probe connections could only be made to the external leads, whereas with unencapsulated cells connections could be made directly to the back metallization. The leads were also fragile in relation to the large mass of the coupon and, despite careful handling, a number of cell leads broke due to repeated bending. Of course lead breakage under these circumstances was not considered a failure mode, but only an artifact of the measurement technique.

3.2 85/85 Test Results

As was discussed in Section 2.3.3, the 85/85 test is a relatively mild test and only small changes were observed when it was applied to

unencapsulated cells. Nevertheless, rather substantial amounts of degradation were observed when encapsulated coupons of these same cell types were tested. This rather anomalous result, which had been alluded to earlier in the 1981 Summary Report (4) as a result of preliminary testing performed on encapsulated cells, has now been confirmed. Table 13 presents the test results in the form of the average percent decrease in maximum power output observed for each of the different encapsulation configurations after 2000 hours total test time. Even recognizing that only a few coupons of each type were involved, a number of effects can be detected. The data of Table 13 will now be discussed on a cell-by-cell basis with conclusions regarding the different encapsulation systems specifically pointed out.

The P- and V-cells showed essentially no degradation for any type of encapsulation. The V-cells had shown little effect when stressed in unencapsulated form, whereas the P-cells had shown somewhat more, with 2 out of 11 cells in the 10 to 19 % degradation range after 1000 hours (See Table 4.). Nevertheless, these two cell types were judged to be very stable in unencapsulated form and remained so when encapsulated. While data for the encapsulated W-cells is not as comprehensive as that for the P- and V-cells, it does not appear that this cell type exhibits any significant amount of degradation when encapsulated either.

> Thus it would appear that a cell which shows little change when stressed in unencapsulated form will be stable when encapsulated, no matter what the encapsulation system.

The Q-cells, on the other hand, showed large degradation for all types of encapsulation except T/EVA/S. This cell when tested in unencapsulated

TABLE 13. Average % Decrease in Maximum Power for Encapsulated Cell Coupons Subjected to 1000 Hours of 85/85 Testing.

	N	O	P	Q	Q	R	V	V	W	X	Y
COUPON	SPR	SPR	SPR	SPR	MFG	SPR	SPR	MFG	SPR	SPR	SPR
G/EVA	---	---	---	---	---	---	---	2	---	---	---
G/EVA/T	31	19	4	42	---	---	-1	1	---	20	-21
G/EVA/F1	15	---	1	53	---	10	---	-1	5	8	-28
G/EVA/F2	---	---	---	---	---	---	---	-2	---	---	---
G/EVA/G	0	---	1	23	---	---	---	---	---	13	-14
G/EMA/T	24	14	1	53	---	---	0	---	---	10	-8
T/EVA/S	-8	5	1*	6	---	---	---	---	2	---	-9
G/SR/G	---	---	---	---	TBS	---	---	---	---	---	---

--- = Tests not planned

SPR = Coupons fabricated by Springborn Labs

MFG = Coupons fabricated by cell manufacturer

TBS = To be started

G = glass, T = Tedlar, F = foil, S = steel, SR = Silicone Rubber

* = all leads off after 1000 hours

form was found to be susceptible to Schottky barrier formation at the back contact (See Section 4.2), and it is believed that the degradation observed on the encapsulated samples was also related to this phenomenon. For this reason a complete discussion of the behavior of encapsulated Q-cells will be delayed until Section 4.2.

> It would also appear that a cell which exhibits a stability problem in unencapsulated form can be significantly improved by use of the "proper" encapsulation system.

The N-cell coupons fabricated with glass or steel hermetic substrates showed no degradation, while those with Tedlar or foil substrates showed appreciable degradation. If the degradation mechanism were activated only by temperature all types of coupons should have degraded more or less equally. The implication therefore is that the N-cells are sensitive to a moisture related degradation mechanism. Furthermore, in those encapsulation systems where degradation was observed it was appreciably greater than had been observed on unencapsulated cells.

> Use of the "wrong" encapsulation system can make an encapsulated cell appreciably more sensitive to environmental stress than an unencapsulated cell.

The N-cell data shows that while the amount of degradation for the foil substrate encapsulation system is less than for the Tedlar substrate system, it is still appreciable. Therefore it must not be water vapor itself which is degrading the cell, since that would be effectively blocked by the metal foil. It is hypothesized that water vapor, which is quite reactive with aluminum, is able to diffuse through the metal film's polymer coating to the foil where it dissociates into hydrogen and oxygen. The oxygen tends to oxidize the aluminum while the hydrogen, which is unable to

escape easily through the polymer film, becomes trapped and increases in concentration at the metal surface. This raises the probability of hydrogen diffusing through the 1-mil thick foil and eventually reaching the metal contact-silicon interface. It is further hypothesized that the presence of hydrogen alters the surface state density at the interface, as will be described in Section 4.2, and results in degradation of the cell. While this exact sequence of events has yet to be proven there is good circumstantial evidence for its occurrence. The point to be made from the data tabulated in Table 13 is that a 1 mil thickness of aluminum, coated with a polymer, apparently does not present much of a diffusion barrier to atomic hydrogen. In addition, aluminum is quite a reactive material. It would be interesting to see if uncoated aluminum foil and foils of other materials, gold for example, might behave differently as would be predicted by the model.

Metal foil, as presently formulated, does not provide an effective barrier against moisture related degradation.

The only cell type, other than the Q, to show any significant amount of degradation when encapsulated in the T/EVA/S configuration was the O-cell. While the amount of degradation was only about one-third that of the other two configurations, the effect was nevertheless felt to be real since all five coupons in the test showed about the same amount of degradation. Degradation did not appear until after 1000 hours, however, and it is surmised that the mechanism in this case was not moisture activated. As seen from Table 2, the O-cell was susceptible to bias-temperature testing and it is felt that the degradation observed during 85/85 testing was more a result of the 85 C temperature rather than of the 85% relative humidity. In addition to Pm degradation this

configuration also showed a 7% drop in Isc while the other O-cell configurations exhibited only small Isc changes.

The only cell type to show a significant amount of degradation when encapsulated in the G/EVA/G configuration, other than the Q-cell, was the X-cell. This cell type was characterized by the loss of grid adhesion (see Section 4.3) and it is felt that this was the dominant failure mode. Loss of grid adhesion in an encapsulated cell is not easily observed, but should result in a reduction in power output as the ohmic metrallurgical contact becomes a pressure contact. Based on hindsight, it would have been interesting to have encapsulated the X-cell in the T/EVA/S configuration to explore the effects of top moisture penetration. As it was, the only encapsulation configurations which were used for this cell had glass superstrates.

The Y-cell in every case showed improvement rather than degradation. From the standpoint of reliability this should not be considered good, however, only different. Examination of the data does not indicate an encapsulation approach capable of minimizing the effect. This is consistant with the unencapsulated results which showed degradation (improvement) to be affected by both heat and humidity.

Althought coupons were visually examined for catastrophic mechanical defects which could be attributed to accelerated testing, none were observed in properly cured samples.

3.3 Thermal Cycle Test Results

Only five samples each of four different types of V-cell coupons, G/EVA, G/EVA/T, G/EVA/F1, and G/EVA/F2, plus one sample of a G/SR/G Q-cell coupon were subjected to thermal cycle testing because of a lack of availability of other types of samples. Very little change was noticed after testing, either electrically or physically, which reinforces the conviction that encapsulation is required to provide mechanical protection. Fracturing had been observed when unencapsulated V-cells where thermal cycled, but not when the coupons were thermal cycled. The Q-cell was sensitive to several forms of mechanical change in unencapsulated form, but no effect was observed when the coupon was tested. The only electrical degradation detected after 40 cycles was 10% on one G/EVA/F coupon and 22% on one G/EVA/G coupon, with none of the others showing any measurable change. Both cells showed progressive degradation after 10 cycles, however. No visual change was observed which could accout for this degradation. The IV characteristics of the two degraded cells indicated the presence of a large shunt resistance. Further work will be required to determine its source.

4.0 DETERMINATION OF FAILURE MECHANISMS

4.0 DETERMINATION OF FAILURE MECHANISMS

4.1 Introduction

As discussed in Sections 2 and 3, accelerated stress testing of both encapsulated and unencapsulated cells resulted in reduced power output. A major goal of the Clemson program is not only to know the magnitude of this degradation and the conditions under which it occurs, but to also discover the underlying physical, chemical, and metallurgical reasons as well. Learning these reasons can be as complicated and involved as tracking down a murder suspect. It calls for following hunches as well as the painstaking use of very sophistocated analytical equipment. In this section we discuss two failure modes that were observed on specific cell types during this round of testing -- Schottky barrier contact formation and loss of grid adhesion. In the case of Schottky barrier contact formation it is felt that the circumstantial evidence that has been accumulated clearly points to the mechanism involved. In the case of the loss of grid adhesion the hunt for the mechanism is still in progress. It is clear from these two examples that determination of degradation mechanisms calls for the latest in microanalytical instrumentation. Clemson is in the process of establishing a reliability research facility containing such equipment and a brief description of the capabilities that will be available is given in this section.

4.2 Schottky Barrier Formation

Most unencapsulated cell types which degraded when subjected to B-T testing did so as a result of an increase in series resistance. This increase caused a decrease in the linear slope of the V-I characteristic in the vicinity of Voc, as shown in Figure 6a. One cell type, the Q-cell, however, developed a distinct non-linearity as shown in Figure 6b. The non-linearity was most pronounced in the far-forward region of the characteristic (V>Voc) and could easily be missed if only the power quadrant were observed. Construction of this particular cell involved a chemical displacement gold film to provide a good plating surface, followed by electroless nickel plating, followed by a solder dip to provide the thick conductive layer. The silicon material was p+ on n. The non-linear shape of the characteristic that was observed after stress testing implied the formation of a rectifying contact, and because the back contact was lightly doped, this would be the most likely location. To simulate this, a discrete Schottky barrier diode was connected to the back of an unstressed cell, with the result shown in Figure 7. Curve A is the unstressed cell characteristic. Curve B is with the Schottky barrier diode connected (connections added about 0.1 ohm series resistance), and because it is unrealistic to expect the back contact to have the right-angle shape of a commercial diode, Curve C is shown in which the diode was shunted by a half-ohm resistor rusulting in a less ideal rectification characteristic. In the power quadrant it can be seen that the effect of the forward diode drop is to push the IV characteristic to lower voltages with a consequent reduction in power output. In the far-forward region only diode leakage

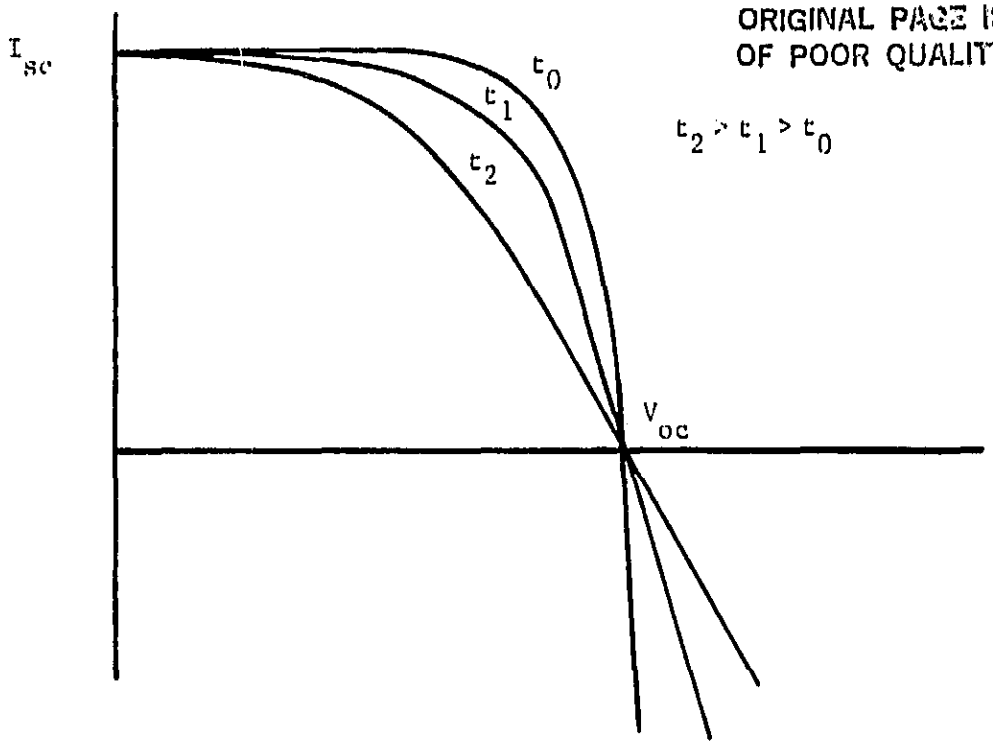

A. LINEAR SERIES RESISTANCE

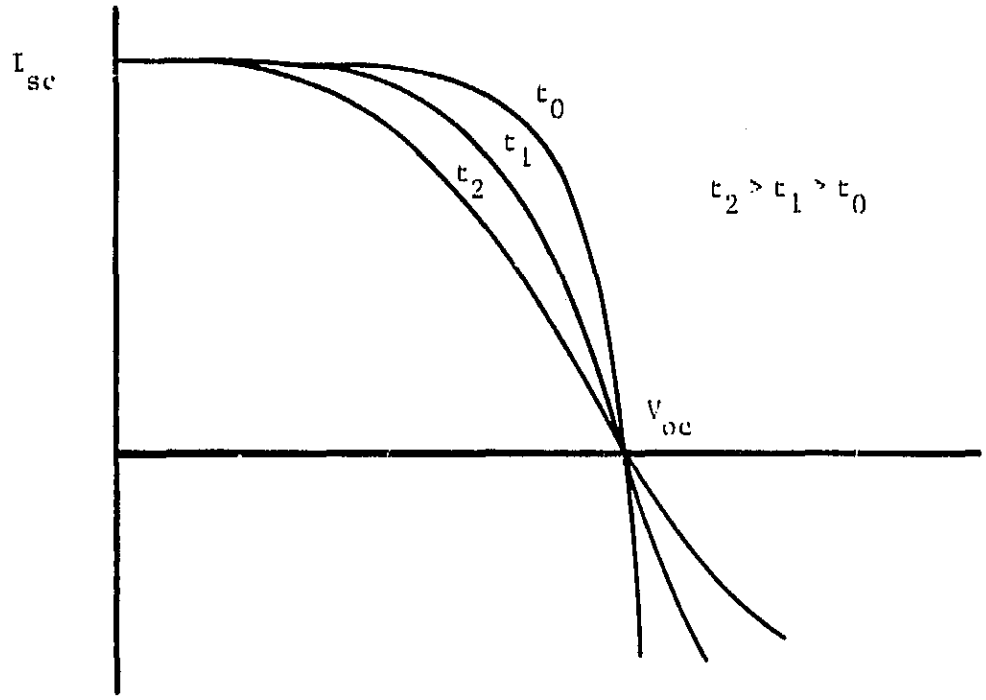

B. NON-LINEAR SERIES RESISTANCE

Figure 6. Typical Characteristics of Cells Subjected to B-T Testing

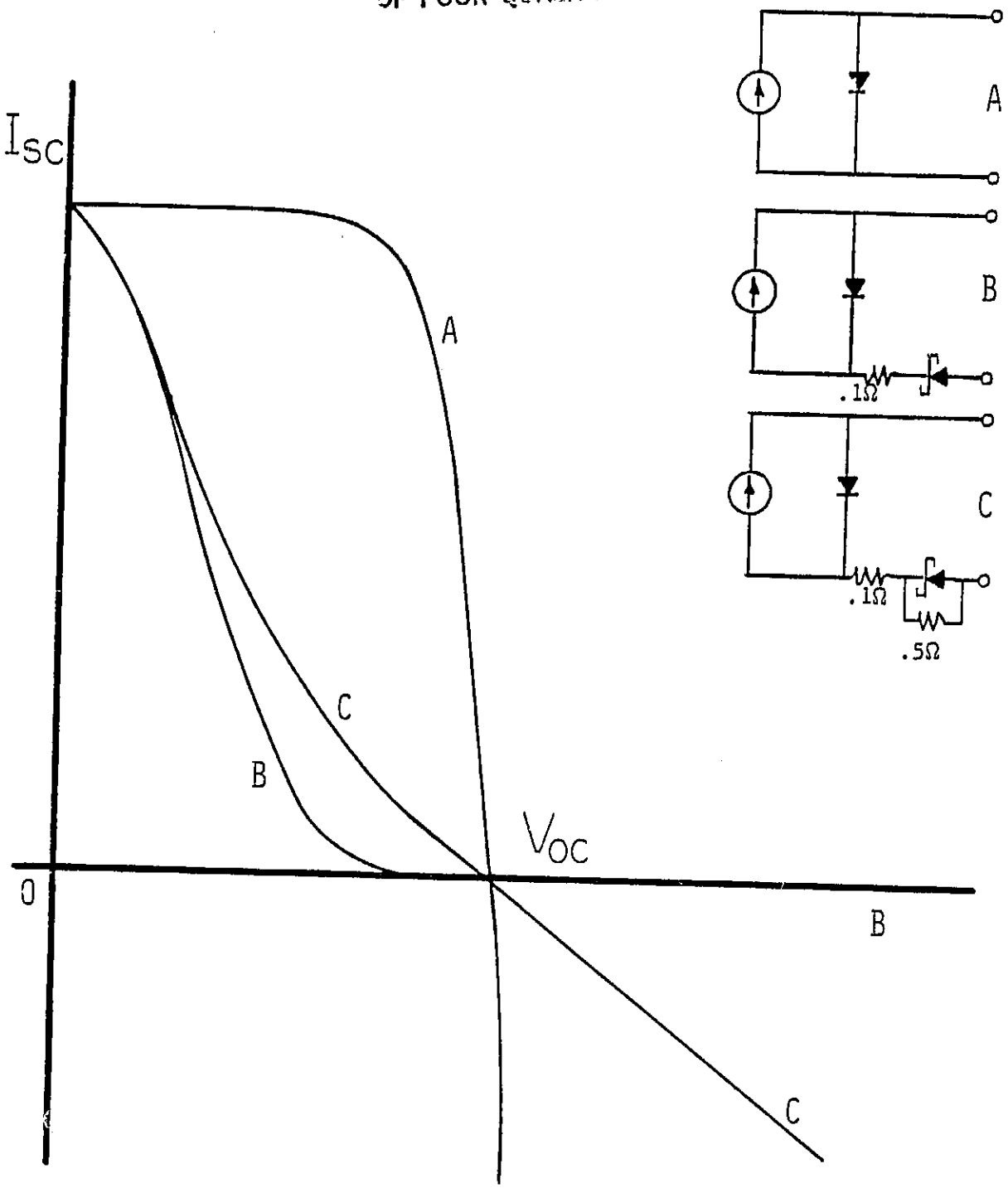

Figure 7. Simulation of Non-Linear Contact Degradation

current flows, or in the case of the shunted diode, current throught the resistor shunt. It can be seen that the shape of Curve C is indeed of the same general non-linear shape as that observed on a stressed Q-cell.

To explore this further the characteristic of a stressed Q-cell was fitted using a computer program, SPICE, and the equivalent circuit of Figure 7 Curve B (without the 0.1 ohm resistor). The result is shown in Figure 8. As had been anticipated, the contact diode characteristic that was required to fit this curve was far from ideal, but enabled a good fit to be obtained.

Most ohmic contacts to solar cells conduct by virtue of quantum mechanical tunnelling. Such tunnelling occurs when the semiconductor is heavily doped, as would be the case with a back surface field. Heavy degenerate doping results in a thin potential barrier that electrons are able to penetrate quantum mechanically. In the case of the Q-cell, however, the base material is not heavily doped and ohmiticity of the contact is achieved by obtaining a low, rather than a thin barrier. It is well known that the rectifying properties of a metal-semiconductor contact are determined largely by the surface states which exist at the interface. The Q-cell achieves its low potential barrier via a damaged surface formed by sandblasting, which serves to provide large quantities of surface states. These surface states, combined with those which would occur naturally at the interface, result in a low, easily surmountable barrier.

The difficulty with this type of contact is that stress conditions occurring in the field (or during laboratory accelerated testing) can

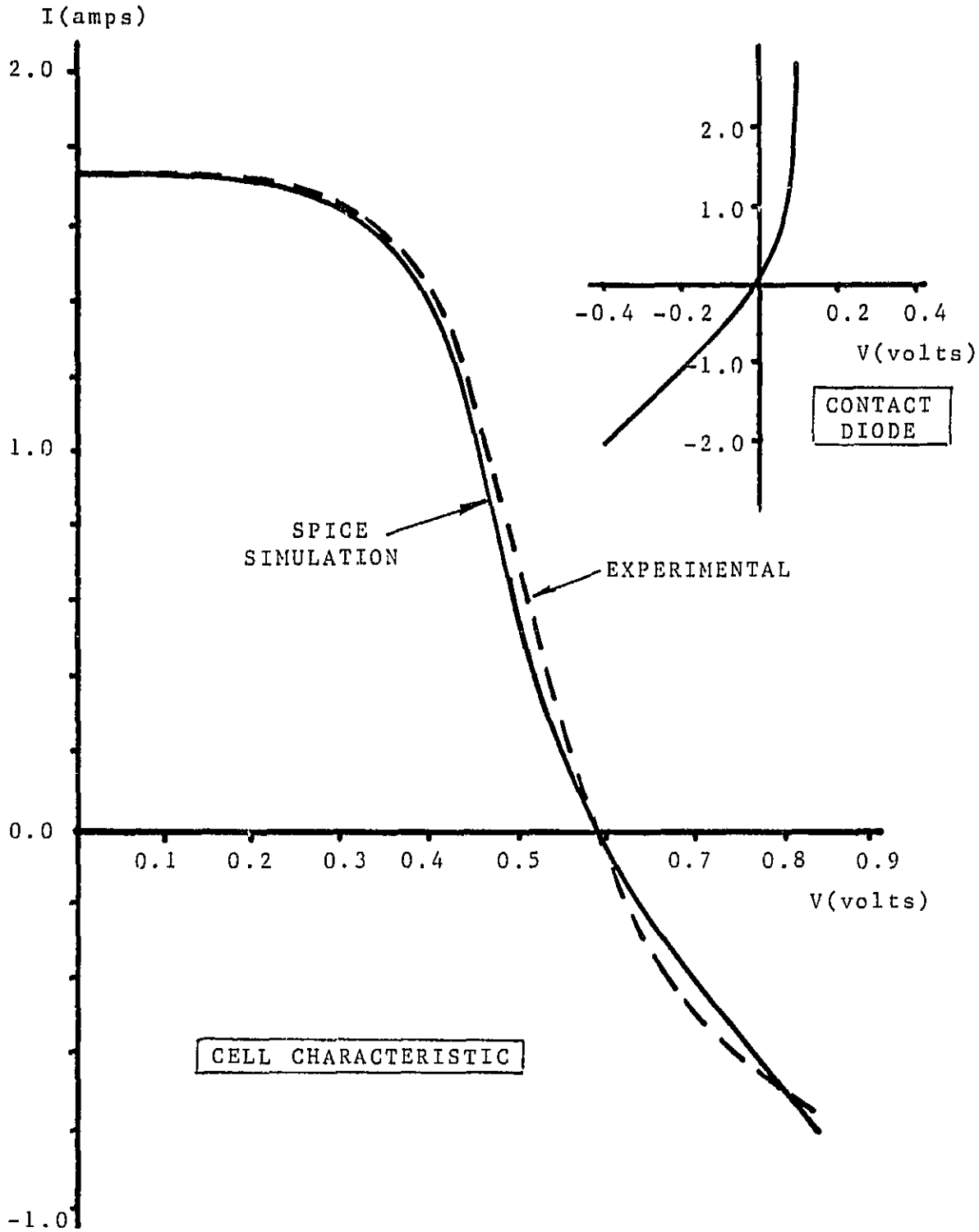

Figure 8. IV Characteristic of a Q-Cell After 600 Hours at 150° as Fitted by SPICE Model Incorporating a Rectifying Circuit

result in a change in the number of surface states. Hence a contact which was originally ohmic may become rectifying, as occurred with the Q-cell. To explain this a theory is proposed based on the fact that surface states are a result of dangling silicon bonds, i.e. silicon valence electrons at the surface that are not shared with electrons from other atoms. At a crystalline surface silicon normally interfaces to the ever present layer of oxide. Experimenters have found that non-stoichiometry occurs in surface oxide films within a few Angstoms of the silicon oxide/silicon interface (6) giving rise to surface states which control the potential barrier height. Furthermore it has been demonstrated that it is possible to control the Schottky barrier height over a wide range by using shallow, highly doped ion implanted layers to achieve a desired degree of bond saturation (7). It should be possible, therefore, for elements in atomic form such as oxygen or hydrogen to diffuse to the interface and to also saturate the dangling silicon bonds, decreasing the number of interface states, raising the barrier height and forming a rectifying contact. It is unlikely that oxygen is the diffusing species, however, since its diffusion coefficient in metals is so small -- of the order of 10E(-23) cm2/sec at 100 C (8). The diffusion coefficient of hydrogen, on the other hand, is 9 or 10 orders of magnitude greater (9, 10, 11). Atomic hydrogen and oxygen can be formed by the dissociation of water vapor molecules at the metal surface. The penetration of hydrogen through metals under high humidity conditions has been reported in the literature (12, 13, 14, 15) and has been found to be strongly dependent on the surface conditions of the metal. Schottky barrier contact formation should take place on lightly doped silicon whenever moisture is present to supply the hydrogen and when the temperature is elevated to increase diffusion to the interface. Indeed non-linear

characteristics were observed on the Q-cell under these conditions. A method of determining the metal to semiconductor barrier height has been developed and is described in Appendix A. Measurements made using this method on typical degraded cells which exhibit non-linearity give a barrier height of 0.55 ev, whereas unstessed cells having ohmic contacts will have a barrier height of approximately 0.3 ev. An experiment which needs to be run and which is currently being planned is to specifically exclude water vapor from the cell environment during B-T testing in order to confirm the role of water vapor.

While further work is expected to shed additional light on the exact mechanisms involved in Schottky barrier formation, it is nevertheless evident that the use of a lightly doped substrate can lead to back contact rectification, and should be avoided. A thin highly doped layer under the back contact has the added advantage of providing a back contact field and thus improving the cell's efficiency.

When either encapsulated or unencapsulated Q-cells were exposed to 85/85 testing, Schottky barrier formation, as evidenced by the formation of a non-linear characteristic, did not occur within the normal 2000 hour time span. Degradation involved an increase in series resistance, but non-linearity in the far forward portion of the characteristic was not discernable. It is hypothesized that the mechanism described above was still valid, but that the test time was too short at this low temperature. The appearance of non-linearity would be expected to occur only after an appreciable increase in the linear series resistance. Non-linearity was not observed in B-T testing at 75 C even after 4800 hours, but was observed in B-T testing at both 150 and 135 C and in pressure cooker testing after 400 hours at 15 psig and 121 C. As the stress temperature is lowered the time to non-linearity gets progressively longer. In order to confirm this, 85/85

testing of the Q-cells is being extended.

Even though non-linearity has not yet been observed during the 85/85 testing of encapsulated Q-cells the degradation which occurred and which is summarized in Table 13 may still be interpreted in terms of the mechanism assumed to lead to non-linearity. Based on the hypothesis that the effect is due to diffusion of hydrogen to the metal/silicon interface, one would expect an encapsulation which hermetically protected the back surface to avoid this degradation mode. Certainly a steel substrate would be expected to give such protection, and did according to the data of Table 13, but what about the glass and foil substrates, which should also offer back contact protection, but apparently didn't? Regarding glass as a substrate material, a closer examination of the data summarized in Table 13 reveals that only three G/EVA/G coupons were started into test and that two of these lost both leads after only 250 hours. The remaining cell showed no degradation until 1000 hours when 19% was observed. Thus the value of 23% degradation shown in Table 13 represents data from only one sample coupon and is still only half the maximum observed for other types of encapsulations for this cell type. Consequently it is felt that the glass substrate probably protected the back surface initially, but that edge diffusion, particularly along the leads, which were sandwiched between two nonconforming surfaces, eventually occurred.

The discussion with regard to the N-cell in Section 3.2 presented a hypothesis as to why the degradation of encapsulated cells with non-hermetic substrates was greater than for unencapsulated cells and why foil substrate material would not protect against hydrogen diffusing to the

metal/semiconductor interface. The amount of hydrogen reaching the interface will depend on the diffusion coefficient of atomic hydrogen in the metal and on the equilibrium surface concentration of atomic hydrogen. If the permeation coefficient of water vapor in the substrate is much greater than for hydrogen, water vapor will diffuse to the metal surface and through dissociation produce hydrogen which will be trapped at the surface. Thus it is possible for the concentration of atomic hydrogen at the metal surface to be greater when the surface is "protected" by a polymeric substrate than when unprotected. The measured permeation coefficient of hydrogen in polyvinyl fluoride is the order of 7E10 molecules per second per cm per atmosphere (16), whereas for water vapor the value is 3.5E13 (17). Thus the permeation coefficient of water vapor in this typical polymer film is 500 times greater than for hydrogen. If atomic hydrogen is able to diffuse to the silicon-silicon dioxide interface, the dangling silicon bonds existing there will become saturated, increasing the surface potential and giving rise to the rectifying Schottky barrier contact. As can be seen from Table 13, degradation in the Q-cell due to Schottky barrier formation is greater for non-hermetic substrates than for unencapsulated cells and is greater for foil substrates than for most of the non-hermetic encapsulation systems.

4.3 Loss of Grid Adhesion

Another clearly identifiable failure mode, pertaining only to the X-cell, which was brought out by the unencapsulated tests was loss of grid adhesion. In an effort to investigate this failure mode further, samples were examined by electron microscopy. It was found that the surface

topology of the X-cell was different from that of many other cells, as can be seen from the 1500X photographs of Figure 9. Figure 9A shows the silicon surface topology after removal of the overlying solder, while Figure 9B shows the mirror image topology of the removed solder. It can be seen that the silicon surface consists of nodules on a gently rolling background. The usually observed structure of silicon after removal of solder, shown in Figure 9C, is much more jagged and irregular without any sign of nodules. When energy dispersive x-ray (EDX) analysis was performed the expected tin and lead from the solder, and nickel from the interface film were found. In addition an appreciable amount of phosphorus, presumably from the nickel plating bath, was present. It is not known at this point, however, if either the surface topology or the presence of phosporus have any relation to the observed loss of grid adhesion. Discussions were held with the manufacturer, who felt the problem involved some unknown contaminant. Additional tests are now being jointly conducted with the manufacturer.

4.4 New Clemson Reliability Research Facility

Clemson University is in the process of establishing a new research facility which will be devoted to fundamental semiconductor device reliability studies. Devices to be studied will range from discrete structures like solar cells to the latest VLSI circuits. The solar cell reliability program will be a major beneficiary of the facility, whose centerpiece is to be the latest in state-of-the-art analytical electron microscopes. This microscope, which is expected to be in operation by the first of the year, is to be installed in a newly constructed room adjacent to Clemson's presently existing Central Electron Microscope Laboratory. In

a) Silicon Surface with Solder Removed (X-cell)

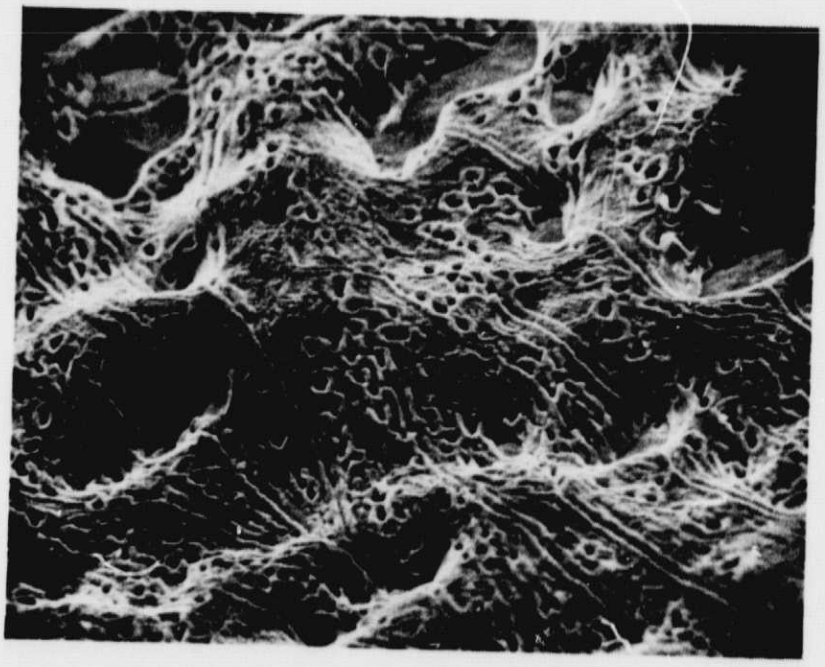

b) Surface of Removed Solder (X-cell)

Figure 9. 1500X SEM Photographs of Cell Surfaces

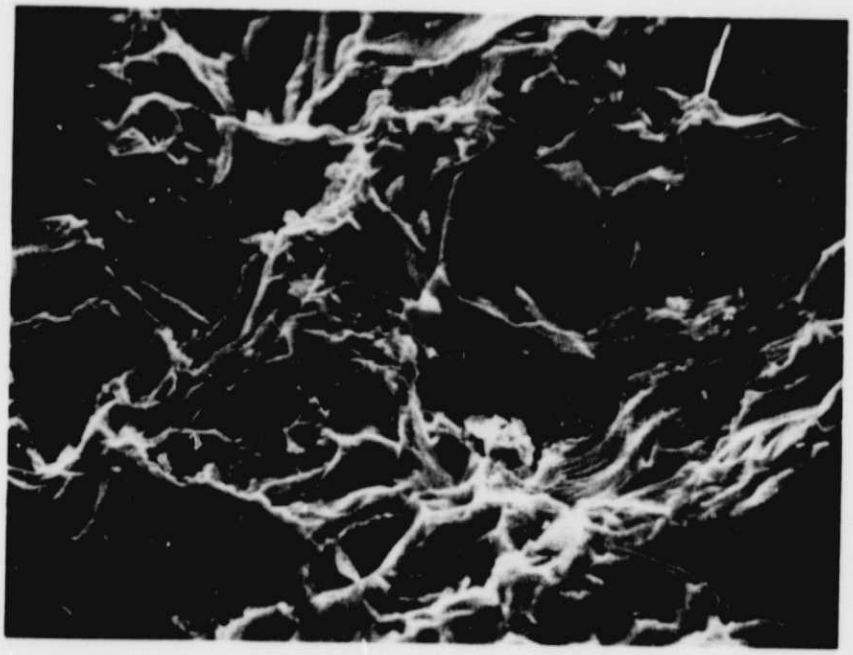

c) Silicon Surface with Solder Removed (not X-cell)

Figure 9. (Continued)

addition to normal high resolution, high depth of focus topological display capability, it will also have the analytical capabilities of a scanning Auger microprobe (SAM) with ion etching for generating depth profiles, an energy dispersive x-ray analyzer (EDX), a secondary ion mass spectrometer (SIM), an electron back scattering analyzer, and all the computerized instrumentation associated with these components. The microscope is expected to be of tremendous help in determining the failure mechanisms responsible for the degradation observed during accelerated testing. In order to acquaint the photovoltaic community with its capabilities a workshop is planned in April 1984, which will include hands-on experience with the instrumentation.

5.0 ADDITIONAL TEST DEVELOPMENT

5.0 ADDITIONAL TEST DEVELOPMENT

5.1 Introduction

A major goal of the program is the development of accelerated tests which can differentiate between different cell constructions in their ability to withstand environmental stress. It has been seen that the 85/85 test is a rather weak test which requires long times before effects are observed. In an effort to develop a similar test with a greater accelerating factor experiments are underway involving variations which include 95 C/85% RH and 85 C/95% RH. The 95/85 test has been started, but it is still too early to draw specific conclusions. After the second downtime, encapsulated V-cells, a cell type which had shown good stability under 85/85 testing, also shows good stability on 95/85 testing. Two additional reliability test techniques are also in the early stages of development -- outdoor real time testing and sulfur dioxide testing. Both of these techniques are being developed in an effort to more closely relate accelerated laboratory testing to real world conditions.

5.2 Outdoor Real-Time Testing

Whereas the testing procedures described in Sections 2 and 3 are impressive in their ability to delineate different failure modes, they offer little information relative to predicing actual operating life. In order to correlate field behavior with accelerated laboratory testing it is first necessary to establish that the same failure modes are being observed

and then to ascertain the acceleration factor. As a first step towards making the accelerated testing to real time connection, Clemson has fabricated fixtures that allow the mounting of both unencapsulated and encapsulated single cells in an outdoor array. Photographs of these arrays are shown in Figure 10. Each unencapsulated cell is mounted on a carrier, that in turn is mounted to a base inclined at the latitude and facing south. Thus using the carrier, cells may be removed from the outdoor base and transported into the lab without demounting and with minimal danger of breakage. A typical cell holder/carrier combination is shown in Figure 11. Originally the unencapsulated cells were mounted in place by clamping their edges, but a freak snowstorm resulted in considerable breakage. As a consequence, the plexiglass holder system of Figure 11 was developed. In addition, a wooden snow cover has been constructed which can be used to cover the array if there appears to be danger of snow. By periodically measuring the cells in the laboratory, under standard conditions of illumination and temperature using the accurate short interval tester, changes in Pm of only a few percent may be determined.

The approach to outdoor real-time testing of using individual cells, coupled with accurate periodic laboratory measurements, is new and has never been investigated before.

It is hoped that changes will be seen which can be related to similar changes observed during accelerated testing. The fear is that extraneous failure modes may prevent the establishment of a correlation, or that under non-accelerated conditions, degradation may take an inordinate length of time. It will be necessary to observe a continuing trend in the degradation which means making observations over an extended period of time. At the writing of this report the array has only recently been set in place and

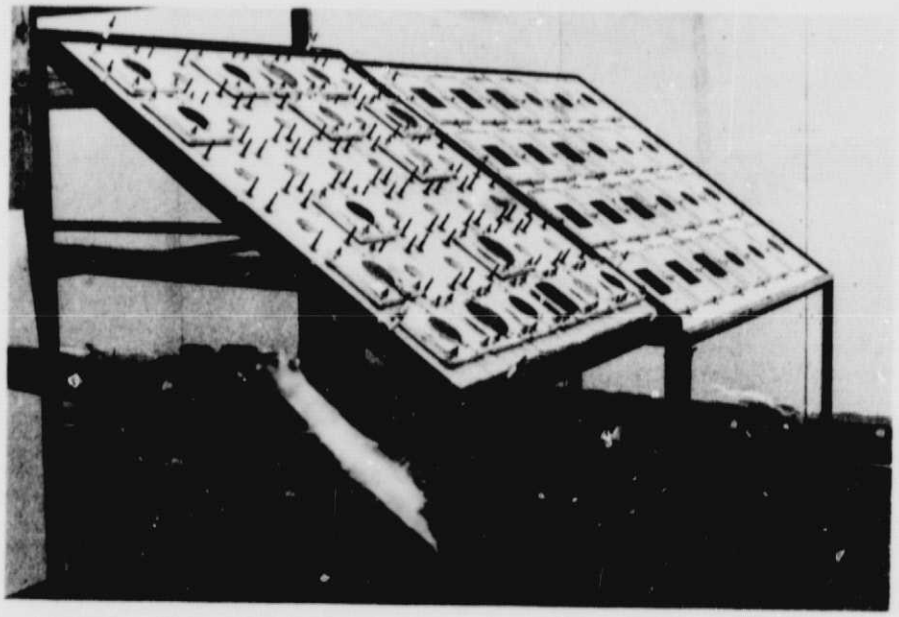

Figure 10. Photograph of Outdoor Real-Time Test Arrays

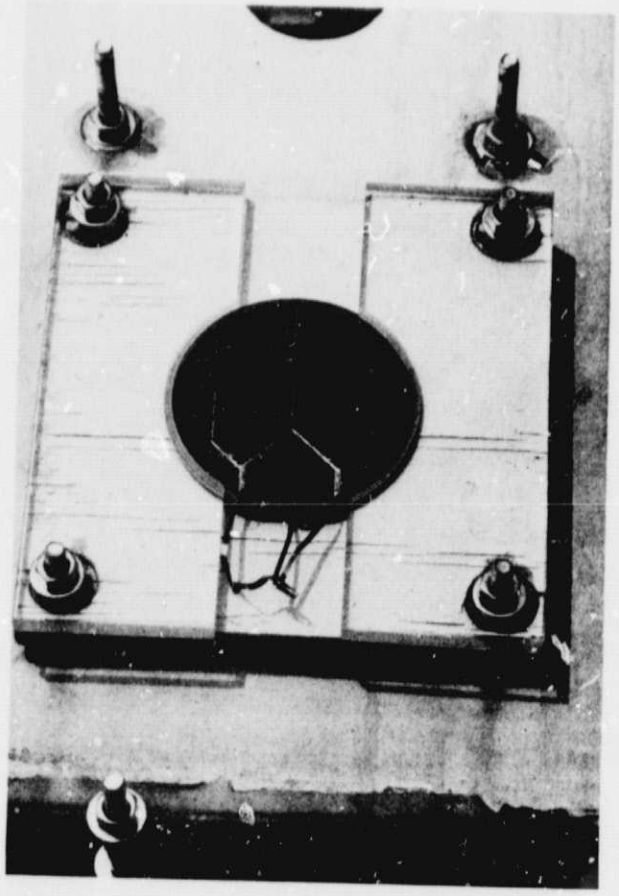

Figure 11. Photograph of Cell Holder/Carrier for Real-Time Test.

data is not yet available.

Cells are mounted so there is a flow of air across both faces. Cell temperature should thus be reasonably close to ambient. The exact value will be checked with thermocouple readings. A portable instrument has been designed and fabricated to measure the cells under actual solar illumination. This instrument measures selected points on the IV characteristic in much the same way as the short interval tester. It is digital and calculates Pm from the data points taken. A comparison of measurements taken in the laboratory and under solar illumination should provide interesting information regarding the presently used ELH lamp simulation method. The cells are loaded individually with a Schottky barrier diode which was determined to more nearly match the cell to its maximum power point than a resistor -- the object being to dissipate the maximum amount of power in the cell. Later, other modifications can be made, such as applying high voltages as may exist in a module between cells at the beginning and end of a series string.

5.2 Sulfur Dioxide Testing

An environmental pollutant which has become of concern recently is sulfur dioxide. Produced primarily by fossil fuel fired power plants, sulfur dioxide combines with the moisture in air in a complex, and as yet not thoroughly understood manner, to produce sulfurous and sulfuric acids which fall to earth as the well publicized acid rain. It is of interest to know whether trace pollutants, such as sulfur dioxide, have an influence on the life of solar cells. Some experimental work on exposing component

metallization systems to SO_2 contaminated atmospheres has been reported in the literature. Feinstein and Sbar (18) identified electrolytic and galvanic corrosion failure modes and also observed the deposition of sulfurous and sulfuric salts. To investigate methods for examining the influence of SO_2 on solar cell performance, Clemson explored methods of establishing and maintaining a humid accelerating test atmosphere containing added amounts of sulfur dioxide up to 500 ppm. It was decided that the base atmosphere should be 85 C and 85% RH to allow easy comparison with previously acquired data. Initially, unencapsulated cells were to be exposed to this ambient and, if correlatable changes were observed, testing would proceed to encapsulated cells. A design study of different methods for producing a steady state 85/85 ambient with trace amounts of SO_2 was performed and is described in Appendix B. The problem proved to be more difficult than anticipated and none of the approaches studied seems appropriate to solar cell testing. It is possible that a closed container test could be designed which used the presence of a measured amount of contaminant. Such a test could be used to differentiate between cell types in their ability to withstand degradation, but would not be relatable directly to field conditions..

6.0 CONCLUSIONS

6.0 CONCLUSIONS

Conclusions can be drawn in a number of specific areas as a result of the work reported in the preceeding sections.

Accelerated Testing Procedures -- The Clemson accelerated test schedule continues to be able to differentiate between cell types in their ability to withstand stress. It is clear that present state of the art cells vary widely in this ability. For routine purposes such as quality control, the testing of unencapsulated cells is more cost effective and time conserving than testing encapsulated cells because because of the ease with thich they may be obtained and because they are able to experience higher temperatures during testing. A research study of encapsulated cell stress sensitivity, such as reported in this document, can make significant contributions to understanding degradation mechanisms, however.

Metallization Systems -- Two previously unreported failure mechanisms relating to metallization systems were uncovered during the course of testing. One, which caused continuous degradation of the maximum power output, is the result of the formation of a rectifying Schottky barrier contact at the back surface of the cell. It is hypothesized that the normally ohmic contact becomes rectifying as a result of hydrogen from the dissociation of water vapor diffusing to the metal-semiconductor interface. Although the non-linearity associated with the formation of a rectifying contact was only observed with one type of cell construction, it is possible that the mechanism accounts for the series resistance related degradation

observed in a number of other cell types. Schottky barrier contact formation could be one manifestation of a more general mechanism which involving changes in the metal - semiconductor barrier height. Another newly discovered failure mode involves the catastrophic loss of contact adhesion. Although the reason for this loss of adhesion is not known, contamination is suspected. Electron microscope photographs reveal a different surface topology for this cell.

Encapsulation Systems -- Encapsulation of any kind protects cells against mechanical problems, such as loss of grid adhesion, which show up during unencapsulated testing. On the other hand, degradation of the back contact, which is most susceptible to moisture related barrier height changes, will be minimized if a hermetic substrate such as steel or glass is used. If a non-hermetic substrate, such as Tedlar, is used degradation is actually increased over that experienced by unencapsulated cells due to its ability to trap hydrogen at the contact - substrtate interface. Furthermore, thin organic coated aluminum film was found to behave essentially as if it were a non-hermetic material for this same reason.

7.0 NEW TECHNOLOGY

7.0 NEW TECHNOLOGY

No items of new technology were uncovered during this reporting period.

8.0 PROGRAM RESEARCH CONTRIBUTIONS

PRECEDING PAGE BLANK NOT FILMED

PAGE 88 INTENTIONALLY BLANK

8.0 PROGRAM RESEARCH CONTRIBUTIONS

Since the previous Annual Report was issued the project has made a number of documented contributions to the photovoltaic community. These are summarized in this section with abstract material reproduced in Appendix C.

Publications and Presentations:

1. Davis, C.W. and Lathrop, J.W., "Electrical Degradation of Solar Cells due to Formation of a Schottky Barrier Contact," Proc. IEEE Region 3 Conference (SOUTHEASTCON), Destin, FL, April 1982.

2. Lathrop, J.W., Hawkins, D.C., Prince, J.L., and Walker, H.A., "Accelerated Stress Testing of Terrestrial Solar Cells," IEEE Transactions on Reliability, Vol. R-31, No.3, p.258, August 1982.

3. Lathrop, J.W., Davis, C.W., and Royal, E., "An Accelerated Stress Testing Program for Determining the Reliability Sensitivity of Silicon Solar Cells to Encapsulation and Metallization Systems," Proc. 16th IEEE Photovoltaic Specialists Conf., San Diego, CA, October 1982.

4. Lathrop, J.W. and Hawkins, D.C., "Degradation of Silicon Solar Cells," Flat-Plate Solar Array Project Research Forum on Quantifying Degradation, Williamsburg, VA, December 1982.

5. Lathrop, J.W., "Accelerated Degradation of Silicon Metallization Systems," Flat-Plate Solar Array Project Research Forum on Photovoltaic Metallization Systems, Callaway Gardens, Pine Mountain, GA, March 1983.

6. White, F.B. and Lathrop, J.W., "Accelerated Reliability Testing of Encapsulated Solar Cells," Proc. IEEE Region 3 Conference (SOUTHEASTCON), p.453, Orlando, FL, April 1983.

Theses:

1. Davis, C.W., "Electrical Degradation of Nickel/Gold and Nickel Metallized Solar Cells Induced by Accelerated Stress," MS Electrical Engineering Thesis, Clemson University, December 1982.

2. White, F.B., "Design of an Accelerated Environmental Test for Solar Cells under Conditions of 85 C, 85% RH, and SO ," MS Electrical Engineering Thesis, Clemson University, December 1983.

Data Exchange:

Computer printouts of electrical measurement data on cells under test was sent to each manufacturer who contributed cells to the program. The manufacturers received information on only their cells, along with interpretive comments, after each down time. The most useful of the printouts was the maximum power output summary listing the performance of each cell in each test. An example of this form is included in Appendix C.

Other:

1. NASA Tech Brief -- The short interval solar cell tester was described in the Spring 1983 edition of NASA Tech Briefs. A copy of the brief is included in Appendix C.

2. Soleras Short Course -- Clara W. Davis, Graduate Student working on the program, was one of 12 US students selected to participate in the 1983 two week summer short course sponsored by the Soleras Program. The US students, together with an equal number of Saudi Arabian students, toured solar installations in the Denver, San Francisco, and Los Angeles areas.

9.0 REFERENCES

9.0 REFERENCES

1. Investigation of Reliability Attributes and Accelerated Stress Factors on Terrestrial Solar Cells, DOE/JPL-954929, 1st Annual Report, May 1979.

2. op. cit., 2nd Annual Report, April 1980.

3. op. cit., 3rd Annual Report, January 1981.

4. op. cit., 1981 Summary Report, June 1982.

5. Saylor, C.R., Lathrop, J.W., and Christ, J.F., "Short Interval Testing of Solar Cells," Proc. 15th IEEE Photovoltaic Specialists Confrence, p.534, Orlando, FL, May 1981.

6. Harrington, W.L. et al, "Low-energy Ion Scattering Spectrometry (Iss) of the SiO2/Si Interface," Applied Physics Letters, vol. 27, p.644 (1975)

7. Shannon, J.M., "Control of Schottky Barrier Height Using Highly Doped Surface Layers," Solid State Electronics, vol. 19, p.537 (1976)

8. Zholobov, S.P., and Malev, M.D., "Diffusion of Oxygen in Metal During Electron Bombardment of a Surface," Zh. Tekh. Fiz., vol. 41, p.627 (1971)

9. Eurinyer, G., "Uber den Zeitlichen Verlaut der Gasabgabe Erhitzter Drahte im Vakuum," Z. Physik, vol. 96, p. 37 (1935)

10. Scherrer, S., Lozes, G., and Deviot, B., "Quenching of Nickel in Hydrogen Atmospheres," C.R. Acad. Sci. B, vol. 38, p. 1436 (1967)

11. Fischer, W., "Kinetics of Hydrogen Permeation through Nickel," Z. Naturfoschg. A, vol. 22, p. 1581 (1967)

12. Cochran, C.N., "The Permeability of Aluminum to Hydrogen," J. Electrochem. Soc., vol. 108, p.317 (1961)

13. Zhukhovitskii, A.A., Gellman, B.G., and Andreev, L.A., "Hydrogen Absorption by Solid Aluminum in Water Vapor," Doklady Akademii Nauk SSSR, vol. 202, p. 1363 (1972)

14. Belyakov, Y.I., Zvezdin, Y.I., and Kurdyumov, A.A., "Penetration of Hydrogen Through Metals which are Oxidized in Steam," Zhurnal Prikladnoi Khimii, vol. 48, p. 981 (1975)

15. Belyakov, Y.I., et al, "Penetration of Hydrogen Through Metals Oxidized in Water Vapor," Zhurnal Prikladnoi Khimii, vol. 49, p.2195 (1976)

16. Ziegel, K.D., Frensdorff, H.K., and Blair, D.E., "Measurement of Hydrogen
Isotope Transport in Poly-(Vinyl Fluoride) Films by the Permeation-Rate Method," Journal of Polymer Science: Part A-2, vol. 7, p.809 (1969)

17. Kellerher, P.G. and Boyle, D.J., "Gaging Moisture Vopor Permeability of Plastic Molding Compounds," Modern Plastics, Nov. 1979.

18. Feinstein, L.G. and Sbar, N.L., "Performance of New Copper-Based Metallization Systems in an 85 C, 78% RH, SO Contaminated Environment," IEEE Trans. Comp., Hybrids, and Mfg. Tech., vol. CHMT-2, p.159, (1979)

APPENDIX A

METHOD OF DETERMINING METAL-SEMICONDUCTOR BARRIER HEIGHT

The saturation current, Is, of a Schottky barrier diode is given by Sze (Ref. 1):

$$I_s = SAT^2 \exp\left(-\frac{q\phi_{Bn}}{kT}\right) \qquad (1)$$

where S = metal contact area

A = effective Richardson constant

ϕ_{Bn} = barrier height

k = Boltzmann's constant

T = absolute temperature

q = electron charge.

Thus the barrier height may be calculated from the saturation current using Equation (1). More accurately, it may be determined from the slope of a plot of ln(Is) vs 1/T.

It of interest to be able to determine the barrier height of a degraded solar cell having a Schottky barrier back contact. The approximate equivalent circuit of such a cell is shown in Figure B1. In this case the Schottky barrier is not directly accessible and it is necessary to deduce the saturation current from the solar cell characteristic. A typical VI characteristic of a degraded cell has 5 distinct regions, as shown in Figure B2. In Region 1 D2, the contact Schottky barrier diode, is fully forward biased while D1, the cell junction diode, is forward biased, but conducting very little (below cutin). The major factor affecting the slope in Region 1 is the shunt resistance. Since this part of the curve is usually nearly horizontal this resistance is large and its effect may be neglected. The

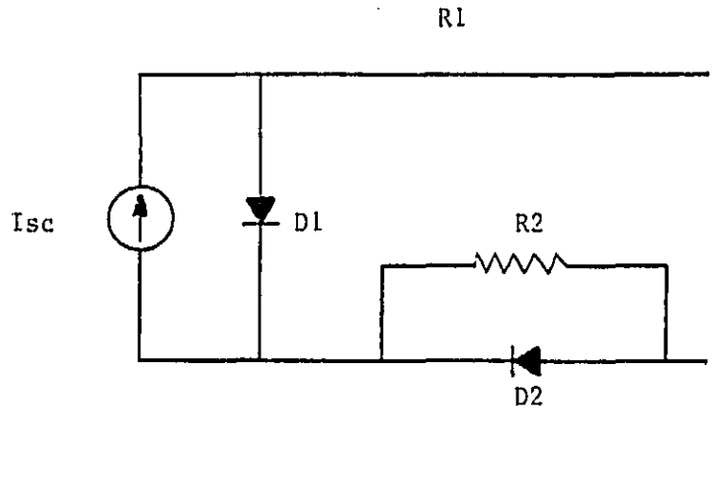

FIGURE B1. EQUIVALENT CIRCUIT OF A DEGRADED SOLAR CELL

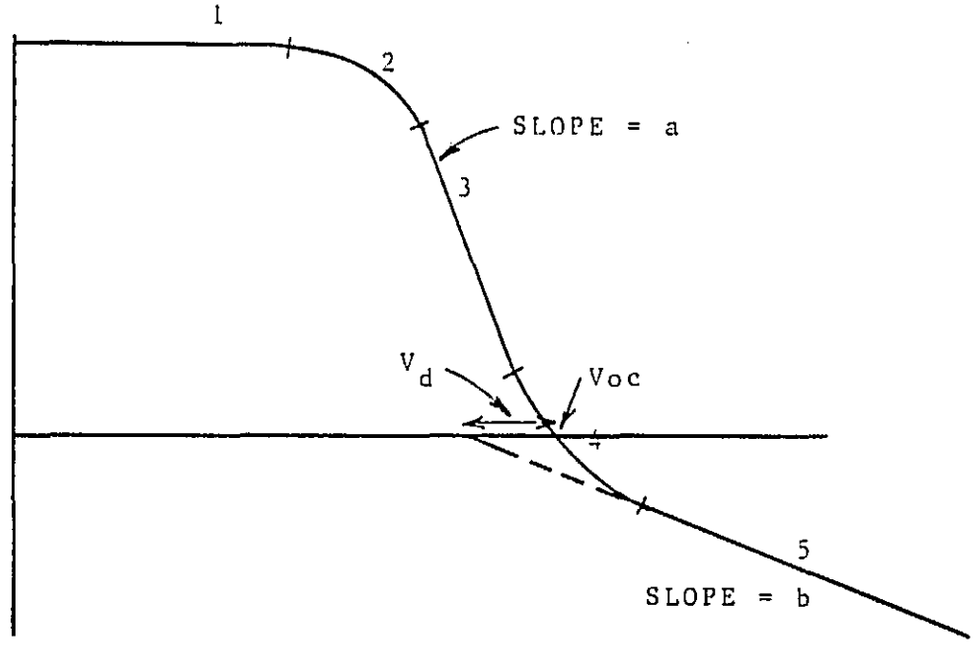

FIGURE B2. VI CHARACTERISTICS OF A DEGRADED SOLAR CELL

concave downward curvature of Region 2 is a result of diode D1 becoming forward biased.

The straight line segment, Region 3, occurs when both D1 and D2 are fully forward biased. Under these conditions the slope of the characteristic, a, is inversely proportional to R1 since R2 is effectively bypassed by D2. The concave upward curvature of Region 4 occurs when D2 drops below its cutin voltage and its conduction current is sharply reduced. In the straight line segment, Region 5, D2 is reverse biased with only saturation current flowing through it while D1 continues to be fully forward biased. In this region the cell's equivalent circuit is given by Figure B3a and Figure B3b (Thevenin equivalent). From Figure B3b it can be seen that the Region 5 slope, b, is inversely proportional to the sum of R1 and R2 and that the voltage difference between its intersection with the voltage axis and Voc is equal to:

$$Vd = Is \times R2,$$

as shown in Figure B2. Thus the saturation current may be determined approximately from the characteristic curve as

$$Is = Vd/((1/b) - (1/a)),$$

where a = slope of Region 3

b = slope of Region 5.

Ref. 1 Sze, S.M., "Physics of Semiconductor Devices," New York: Wiley-Interscience (1981) p. 262.

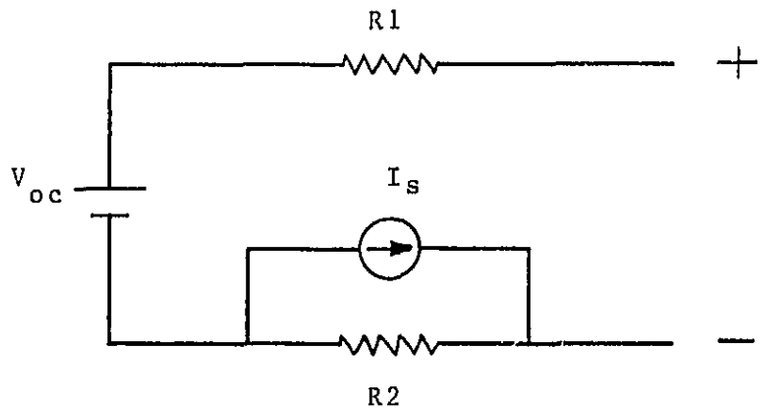

(a) Equivalent Circuit

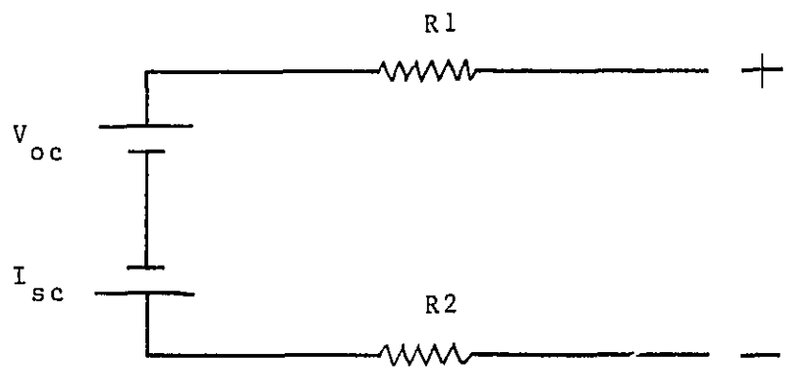

(b) Thevenin Equivalent

FIGURE B3. EQUIVALENT CIRCUIT OF DEGRADED SOLAR CELL IN REGION 5.

APPENDIX B

DESIGN CONSIDERATIONS FOR A CONSTANT FLOW SO_2 ACCELERATED TEST SYSTEM

Appendix B.

Design Considerations for a Constant Flow SO_2 Accelerated Test System

Five methods were considered as ways of producing an 85/85 atmosphere contaminated with SO_2 for stressing cells. These methods, shown in Figures B1 through B5, were considered in regard to effectiveness, ease of control, and concentration range. (Refer to Figure B6 for the list of symbols.) The first design (Figure B1) incorporated a premixed 500 ppm SO_2 source. Since this design did not dilute the premixed source with air, environmental control was simple. However, in order to obtain 85% RH the SO_2 would have to bubble through water. This was not practical since the water would absorb the SO_2.

The second design (Figure B2) also used a premixed source, but one which had a concentration of 1000 ppm, the highest concentration readily commercially available. This allowed the source gas to be diluted with humidified air at the test temperature, thus avoiding the problem of SO_2 adsorption in the humidifier. Concentration control was obtained through the use of flow meters making control simple and accurate. Unfortunately the maximum concentration possible with this system was 150 ppm, but it should be considered a candidate if lesser concentrations are desired.

The third design (Figure B3) was an attempt to avoid this concentration limitation by reducing the flow of the diluting air stream and at the same time raising its humidity. Control now depended on the temperature of

saturation and in maintaing the saturated gas flow at this temperature to the point of mixing. The advantage of flow meter contol of concentration was lost, however, and this approach was not considered practical.

The fourth design (Figure B4) used a pure SO_2 source, which was liquid at room temperature and 34 psig. If conventional flow meters were used for control, the amount of SO_2 was too large resulting in a minimum chamber concentration on 2000 ppm. This approach should be considered if a controllable flow meter and valve combination can be found which will regulate to 1 mlpm.

The fifth design configuration (Figure B5) also used a pure SO_2 source, but a capillary tube was introduced in the SO_2 line to reduce the flow rate. Unfortunately flow through a capillary cannot be monitored as through a flow meter, but when used in connection with a micro metering valve it can be calibrated. This approach was deemed the most feasible of the five constant flow methods for conducting initial investigations and experimental construction was initiated. Results were inconclusive, however, because no satisfactory method of monitoring the SO_2 concentration could be found to insure that the cells were actually being subjected to the desired ambient.

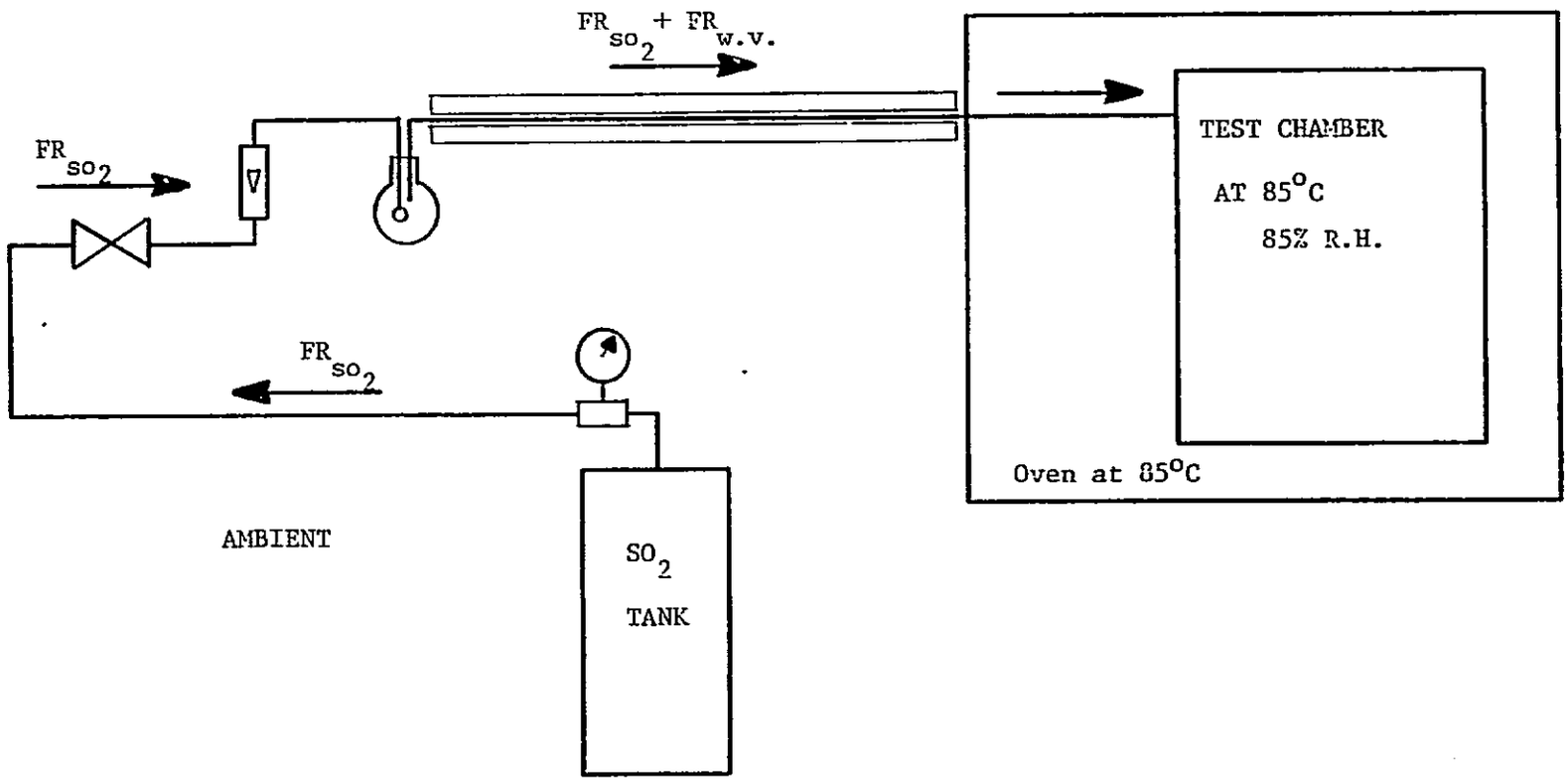

Figure B1. Sulfur Dioxide Test Type A

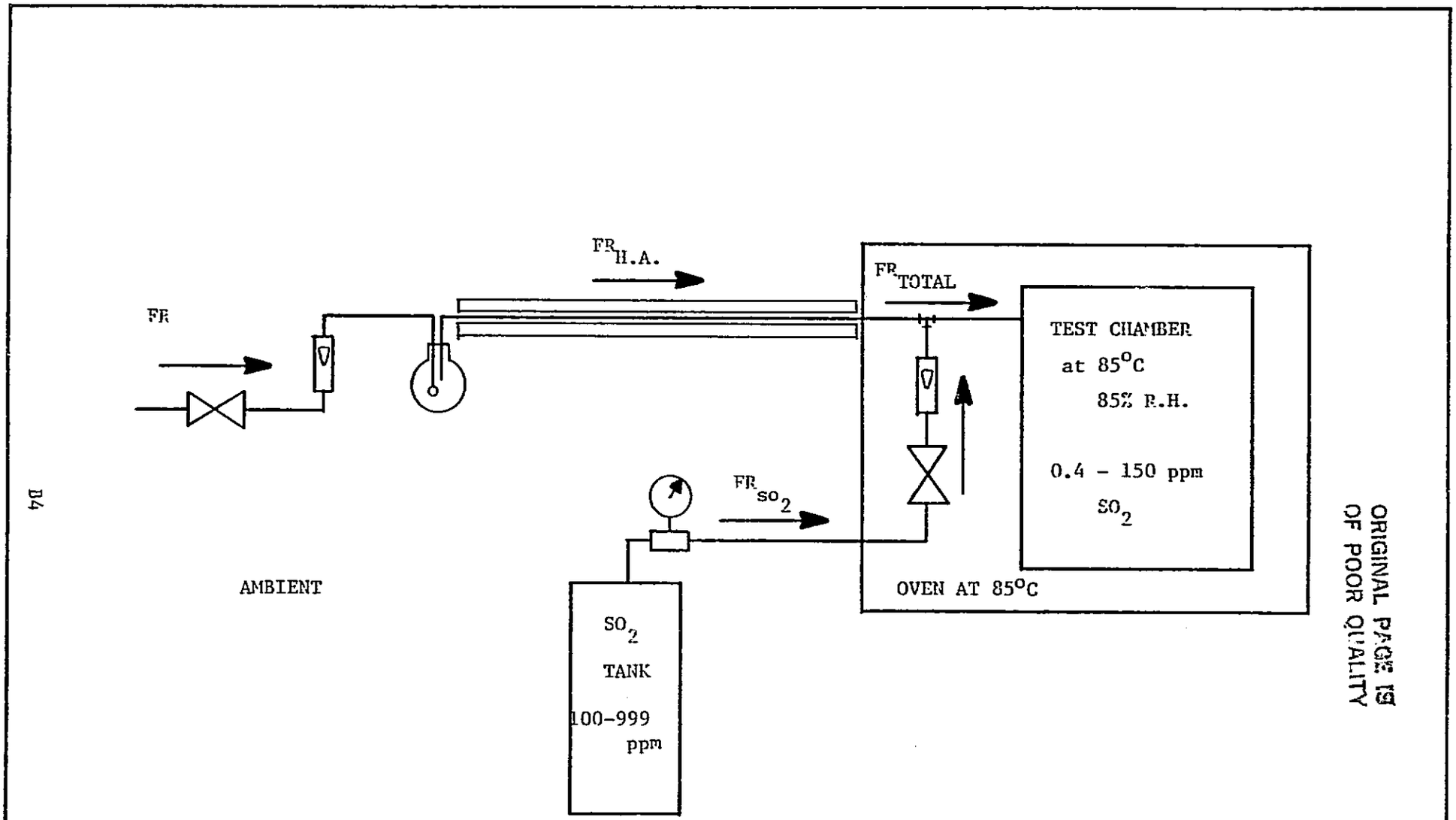

Figure B2. Sulfur Dioxide Test Type B

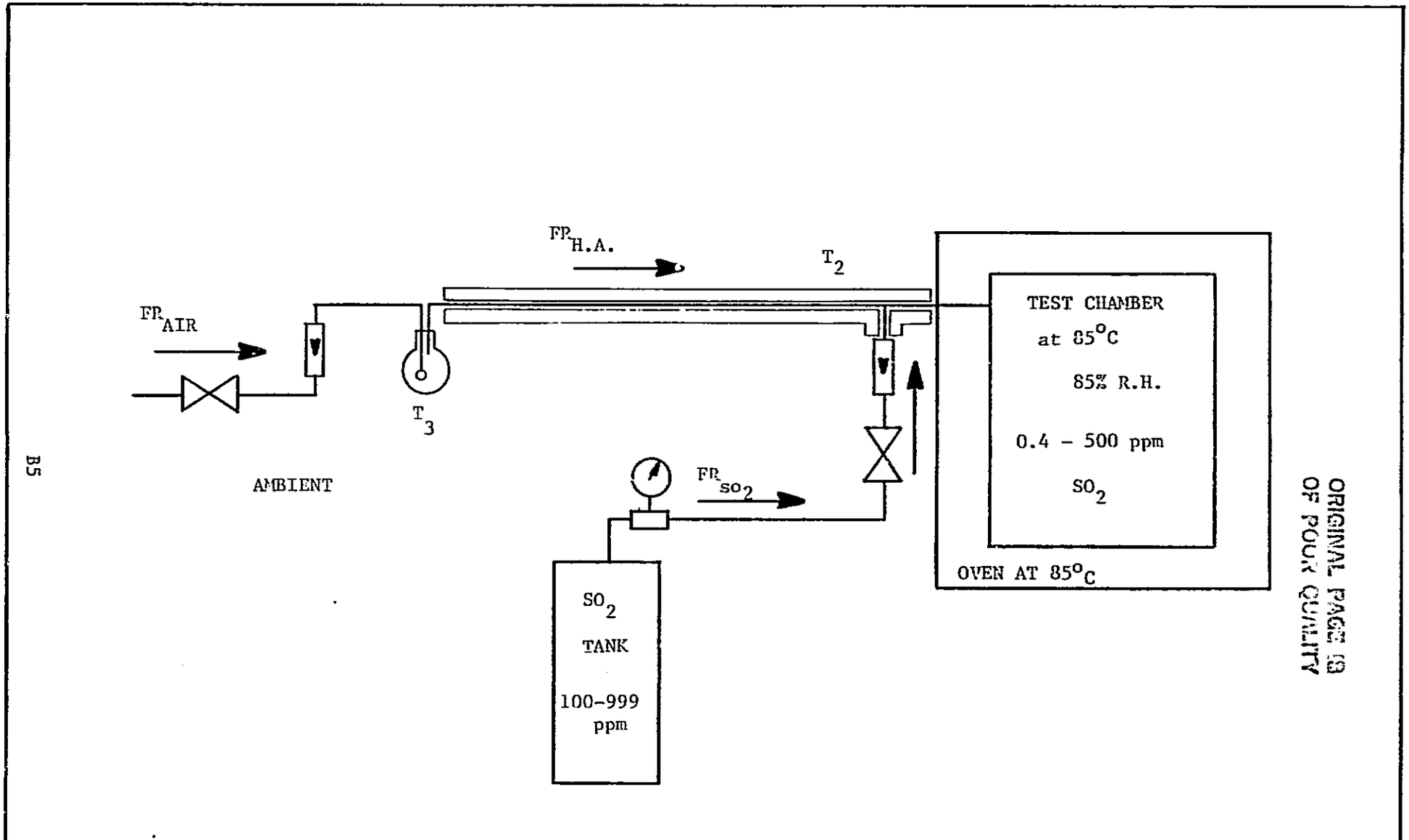

Figure B3. Sulfur Dioxide Test Type C

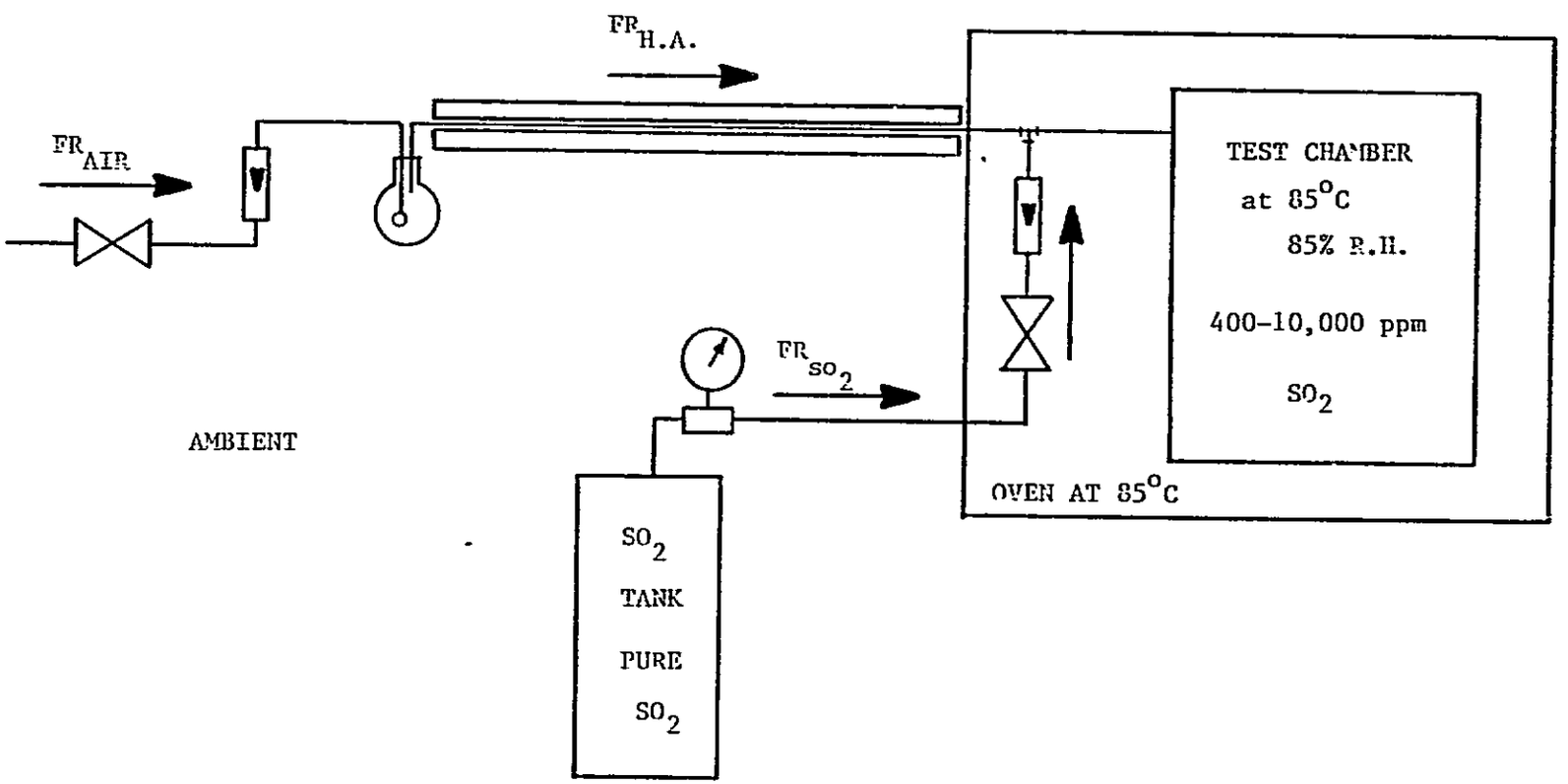

Figure B4. Sulfur Dioxide Test Type D

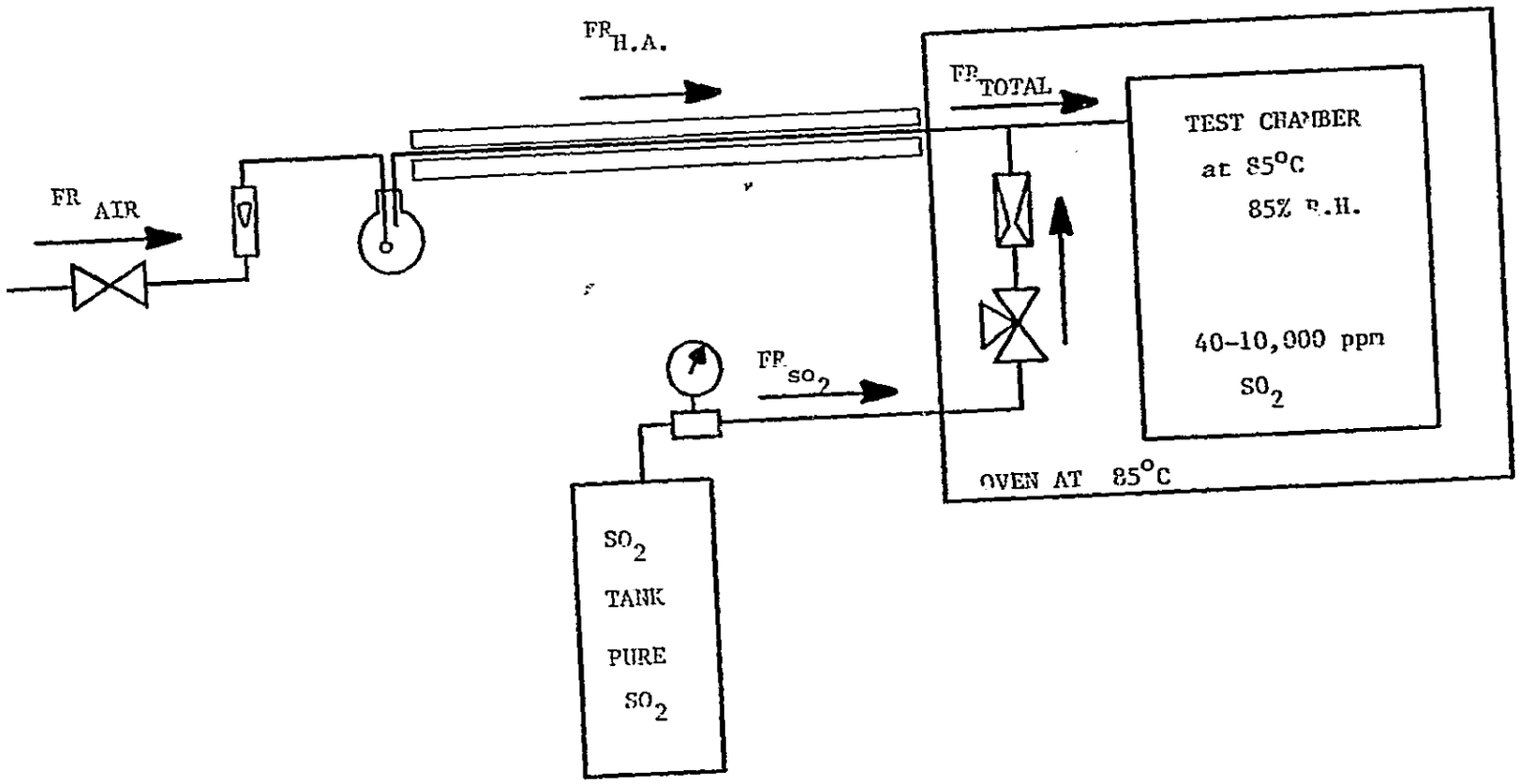

Figure B5. Sulfur Dioxide Test Type E

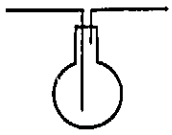

1) water bubbler

5) Auto transformer

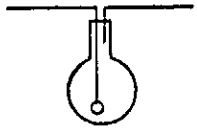

2) water bubbler with fritted disk

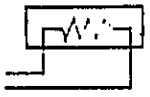

6) hot plate

3) hemispherical heater

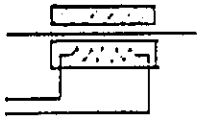

7) heating tape

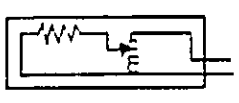

4) auto-transformer controlled hot plate

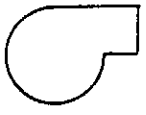

8) blower

Figure B6. Key to Drawing Symbols

9) Pressure Regulator

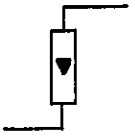

12) Flow Meter

10) Air Purifier
(4 to 5 μm)

13) Micrometering Valve

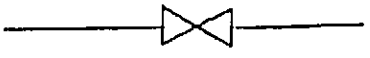

11) Flow Valve

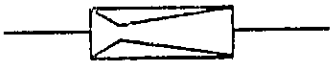

14) Capillary Tube

15) Tee Connector

Figure B6. Key to Drawing Symbols (continued)

APPENDIX C

PUBLICATION ABSTRACTS

Proc. IEEE Region 3 Conference, p.411 (1982)

Electrical Degradation of Solar Cells due to Formation of a Schottky Barrier Contact

C.W. Davis
J.W. Lathrop

Department of Electrical and Computer Engineering
Clemson University, Clemson, SC 29631

ABSTRACT

A decrease in the maximum power output of silicon solar cells subjected to bias-temperature stress testing has been observed. An explanation for this degradation is offered which involves the formation of a potential barrier at the metal-silicon interface of the back contact. The samples used were four-inch diameter silicon solar cells with Au/Ni/Solder contacts. These samples were heated in air to temperatures of 165 C for as long as 9000 hours. Changes in the electrical properties with respect to time and temperature were recorded. Increases in series resistance and nonlinearity of the far-forward characteristic of the cells indicated the presence of a potential barrier. A computer model was developed which included a diode in series with the solar cell. Decreasing the reverse saturation current of the series diode resulted in a more nonlinear far-forward response of the system.

IEEE Trans. on Reliability, Vol. R-31, p.258 (1982)

Accelerated Stress Testing of Terrestrial Solar Cells

J.W. Lathrop, D.C. Hawkins, J.L. Prince, and H.A. Walker

Department of Electrical and Computer Engineering
Clemson University, Clemson, SC 29631

ABSTRACT

The development of an accelerated test schedule for terrestrial solar cells is described. This schedule, based on anticipated failure modes deduced from a consideration of IC failure mechanisms, involves bias-temperature testing, humidity testing (inclding both 85/85 and pressure cooker stress), and thermal-cycle thermal-shock testing. Results are described for 12 different unencapsulated cell types. Both gradual electrical degradation and sudden mechanical change were observed. These effects can be used to discriminate between cell types and technologies relative to their reliability attributes. Consideration is given to identifying laboratory failure modes which might lead to severe degradation in the field through second quadrant operation. Test results indicate that the ability of most cell types to withstand accelerated stress testing depends more on the manufacturer's design, processing, and workmanship than on the particular metallization system. Preliminary tests comparing accelerated test results on encapsulated and unencapsulated cells are described.

Proc. 16th Photovoltaic Specialists Conference, p. 1262 (1982)

An Accelerated Stress Testing Program for Determining the Reliability Sensitivity of Silicon Solar Cells to Encapsulation and Metallization Systems

J.W. Lathrop, C. W. Davis
Department of Electrical and Computer Engineering
Clemson University, Clemson, SC 29631

and

E. Royal
Jet Propulsion Laboratory
Pasadena, CA 91109

ABSTRACT

The use of accelerated testing methods in a program to determine the reliability attributes of terrestrial silicon solar cells is discussed. Different failure modes are to be expected when cells with and without encapsulation are subjected to accelerated testing and seperate test schedules for each are described. Unencapsulated test cells having slight variations in metallization are use to illustrate how accelerated testing can highlight different diffusion related failure mechanisms. The usefulness of accelerated testing when applied to encapsulated cells is illustrated by results showing that moisture related degradation may be many times worse with some forms of encapsulation than with no encapsulation at all.

Flat-Plate Solar Array Project Research Forum on Quantifying Degradation
Williamsburg, VA December 1982

Degradation of Silicon Solar Cells

J. W. Lathrop and D.C. Hawkins

Department of Electrical and Computer Engineering
Clemson University, Clemson, SC 29631

ABSTRACT

Results of the Clesmon accelerated test program are reviewed. Examples of the way in which accelerated testing can be used to differentiate between different cell constructions are given for both encapsulated and unencapsulated cells. A modest real time test program which has been begun in an attempt to correlate field degradation with accelerated test degradation is described. In this program individual cells, both encapsulated and unencapsulated, are stressed outside, but periodically demounted and accurately measured in the laboratory. Development of non-linear VI characteristics in some cells during accelerated testing is discussed. Testing is described in which degradation occurs more rapidly when cells are encapsulated than when they are unencapsulated.

Flat-Plate Solar Array Project Research Forum on Metallization Systems
Calaway Gardens, Pine Mountain GA, March 1982

Accelerated Degradation of Silicon Metallization Systems

J. W. Lathrop

Department of Electrical and Computer Engineering
Clemson University, Clemson, SC 29631

ABSTRACT

The different metallization systems that have been investigated in the Clemson accelerated test program are reviewed. It is shown that all metallizations fall in one of four classifications: vacuum depositied silver, electroplated copper, screen printed silver frit, or solder coated nickel. The number and function the layers in each system is described. A particular cell construction which exhibited non-linear behavior after accelerated testing is examined in detail. Metal to semiconductor contact theory is reviewed and it is concluded that this non-linear behavior is a result of a change in the number of interface states. These interface states are the result of dangling silicon bonds -- electrons which are not shared between silicon atoms at the surface and oxygen atoms in the silicon oxide surface film. A decrease in the number of states, as might occur through the diffusion of atoms capable of sharing electrons to the interface, will cause an increase in the potential barrier at the interface and give rise to a poorly rectifying contact -- a Schottky barrier contact. The formation of this contact appears to be more a function of the semiconductor doping than of the particular metallization system used.

Proc. IEEE Region 3 Conference (SOUTHEASTCON) p.453 (1983)

Accelerated Reliability Testing of Encapsulated Solar Cells

F.B. White and J.W. Lathrop

Department of Electrical and Computer Engineering
Clemson University, Clemson, SC 29631

ABSTRACT

Various types of encapsulated systems with electrically biased solar cells were subjected to an environment of 85 C and 85% relative humidity. The encapsulation systems have been categorized into three groups: bare cells, hermetic substrates, and non-hermetic substrates. The non-hermetic substrates degraded the worst while the hermetic substrates degraded the least.

Fast Electronic Solar-Cell Tester

Microcomputer-controlled system gathers current and voltage data.

NASA's Jet Propulsion Laboratory Pasadena California

A microcomputer-controlled system measures solar-cell current/voltage (I/V) characteristics and determines key cell parameters, including short-circuit current; voltage, current, and power at the maximum-power point; and open-circuit voltage. A cell is automatically stepped through a sequence of electrical loads that increase from open-circuit to short-circuit, while the system measures the cell voltage and computes the power output. The data are displayed on a cathode-ray tube (CRT), recorded on an X-Y plotter, or stored on tape.

The system is illustrated in the figure. A shutter between the lamp and the cell reduces the exposure time and minimizes heating. Heating is further reduced by a dichroic reflector, which directs mostly visible light onto the cell while permitting much of the infrared light to escape. The cell is also cooled by forced air circulation.

Each load is applied to the cell by a programable dc power supply. Following the voltage measurement at each current setting, the microcomputer repeats and verifies the voltage measurement and computes the power output. The microcomputer steps the solar cell through approximately 200 test loads each second.

Data are obtained with three test sequences: In an initial sequence, dV/dI is determined at I = 0 followed by the measurement and verification of voltages at increasing currents in increments of 32 mA. Power is computed at each test point and compared with the previous value.

Upon detection of a decrease in power output, the program jumps to a sequence that decrements current by 1 mA until the maximum-power point has been passed again. The program then jumps to a third sequence that resumes the current stepping but with increments that are varied to maintain the voltage increments between 1.2 and 19.5 mV. The measurements continue until the plateau region of the I/V curve is completely mapped to the short-circuit (V = 0) point.

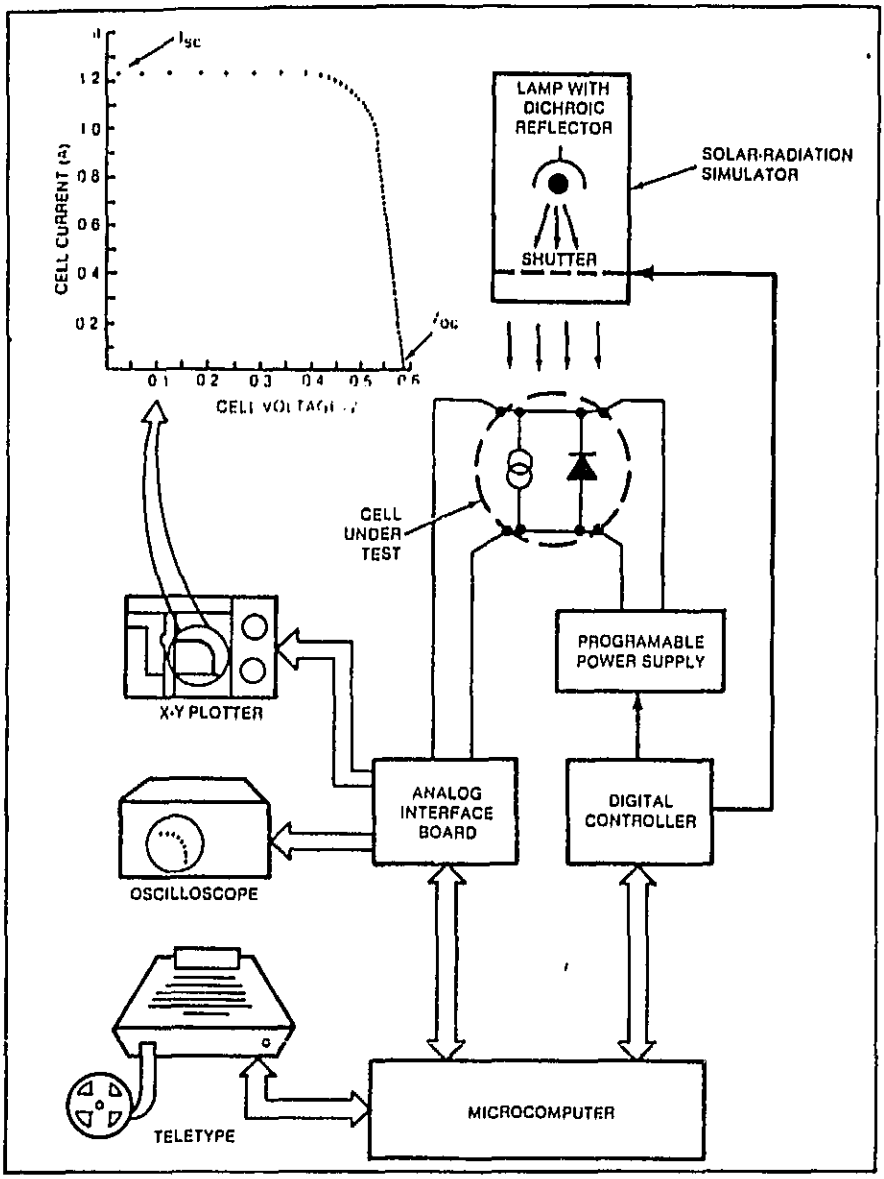

The Programmable Photovoltaic-Cell Test System consists of a light source, microcomputer, programable dc power supply, analog/digital interface, and data storage and display equipment. The system applies a series of test loads to the cell via the programable dc power supply to obtain the I/V characteristic curve and key cell-performance parameters.

The system tests a wide range of solar cells. The apparatus and programing technique are also applicable to other devices, such as other types of batteries and sensors.

This work was done by Jay W. Lathrop and Charles R. Saylor of Clemson University for **NASA's Jet Propulsion Laboratory.** *For further information, Circle 9 on the TSP Request Card.*
NPO-15676

PERCENT DECREASE IN PM CELL BY CELL

PCDX = % DECREASE OF PM AFTER X STRESS LEVELS

TYPE=0 LOT=11

OBS	CELLNO	PM0	PM1	PCD1	PM2	PCD2	PM3	PCD3
346	26	0.759	0.682	10.145	0.653	13.966	0.325	57.181
347	27	0.753	0.649	13.811	0.610	18.991	0.130	82.736
348	28	0.716	0.602	15.922	0.576	19.553	0.082	88.547
349	29	0.738	0.645	12.602	0.616	16.531	0.113	84.688
350	30	0.755	0.626	17.086	0.604	20.000	0.065	91.391
351	31	0.743	0.632	14.939	0.610	17.900	0.092	87.618
352	32	0.738	0.588	20.325	0.572	22.493	0.061	91.734
353	33	0.757	0.690	8.851	0.669	11.625	0.081	89.300
354	34	0.733	0.594	18.963	0.576	21.419	0.084	88.540
355	35	0.774	0.637	17.700	0.615	20.543	0.057	92.636
356	36	0.734	0.613	16.485	0.594	19.074	0.067	90.872
357	37	0.771	0.681	11.673	0.667	13.489	0.076	90.143
358	38	0.804	0.717	10.821	0.704	12.438	0.074	90.796
359	39	0.738	0.594	19.512	0.579	21.545	0.054	92.683
360	40	0.759	0.627	17.391	0.613	19.235	0.083	89.065
361	41	0.755	0.633	16.159	0.609	19.338	0.533	29.404
362	42	0.755	0.638	15.497	0.621	17.748	0.585	22.517
363	43	0.757	0.610	19.419	0.588	22.325	0.359	52.576
364	44	0.825	0.643	22.061	0.580	29.697	0.177	78.545
365	45	0.807	0.705	12.639	0.692	14.250	0.373	53.779

Example of Pm Data Printout Transmitted to Manufacturers